Myogenic and Functional Effects of Deflazacort Therapy on *mdx* Dystrophic Mice.

By

Michael H. Weber

A Thesis Submitted to the Faculty of Graduate Studies in Partial Fulfillment of the Requirements for the Degree of

Master of Science (M.Sc.)

Department of Human Anatomy and Cell Science
University of Manitoba
Winnipeg, Manitoba

THE UNIVERSITY OF MANITOBA

FACULTY OF GRADUATE STUDIES

*****

COPYRIGHT PERMISSION PAGE

Myogenic and Functional Effects of Deflazacort Therapy on *mdx* Dystrophic Mice

BY

Michael H. Weber

A Thesis/Practicum submitted to the Faculty of Graduate Studies of The University of Manitoba in partial fulfillment of the requirements of the degree of Master of Science

Table of Contents

Abstract

Duchenne muscular dystrophy (DMD) is caused by a lack of dystrophin. *Mdx* dystrophic mice experience acute and extensive muscle fiber necrosis at 3wks-of-age, followed by regeneration with little disability. Early treatment with deflazacort, a glucocorticoid, slows dystrophy and improves repair. While the mechanism of action is unknown, effects on repair may be due to increased proliferation by myogenic precursor cells (mpc) or more recruitment to the cell cycle. Expression of myogenic regulatory factor gene transcripts in cells identified as mpc can be studied using *in situ* hybridization (ISH). Along with labels for DNA synthesis, changes in mpc proliferation can be determined. Deflazacort may also increase laminin expression that could stabilize new fibers. We hypothesized that deflazacort treatment benefits function and promotes repair by increasing mpc proliferation and fiber differentiation. *Mdx* mice (3.5wks) were treated with deflazacort (1.2mg/kg) for 4wks while muscle strength was measured regularly. A crush injury was given to one tibialis anterior muscle, and four days later, muscle was collected to study creatine kinase (CK) isoforms, mpc proliferation and laminin expression. *Mdx* strength increased with deflazacort in correlation with a shift of CK isoforms to a more mature MM isoform. ISH/autoradiography experiments showed increased proliferation by myogenin+ but not MyoD+ mpc. Laminin mRNA and protein expression were increased (Northern and Western blots) by deflazacort treatment. Hence, deflazacort promoted functional gains and myogenic differentiation in regenerating dystrophic muscle, and these findings encourage future studies to optimize early treatment of DMD.

Acknowledgments

I would like to recognize and thank my supervisor Dr. Judy Anderson for her confidence and assistance with my studies both in and out of the lab. I would like to thank the members of my advisory committee, Dr. Cooper (School of Medical Rehabilitation), and Dr. Kardami (Department of Human Anatomy and Cell Science) for their support with this project. I would also importantly like to thank the Department of Human Anatomy and Cell Science for its people and resources.

I would also like to acknowledge the valuable technical expertise and assistance of Cinthya Vargas. In addition, I would like to thank Dr. Triggs-Raine (Department of Biochemistry and Molecular Biology) and her technician Tim Salo for their work on the CK isozyme gels. The cDNA for α2-laminin, was a gift from Dr. Eva Engvall (La Jolla Cancer Research Centre, The Burnham Institute). A grant from the Muscular Dystrophy Association U.S.A. to Dr. Anderson supported these investigations.

List of Abbreviations

(ATP)	Adenosine Triphosphate
(ANOVA)	Analysis of Variance
(RAG)	Autoradiography
(bHLH)	basic Helix-Loop-Helix
(BSA)	Bovine Serum Albumin
(BrdU)	Bromodeoxyuridine
(c-terminal)	Carboxyl-terminal
(C)	Control C57BL/10 mice
(CK)	Creatine Kinase
(DAB)	Diaminobenzidine
(DIA)	Diaphragm
(DEPC)	Diethyl Pyrocarbonate
(DIG)	Digoxigenin
(2x, 1x)	double or single concentration
(DMD)	Duchenne Muscular Dystrophy
(DAG)	Dystrophin-Associated Glycoprotein
(DAP)	Dystrophin-Associated Protein
(EDTA)	Ethylenediaminetetracetic Acid
(FGF)	Fibroblast Growth Factor
(Ht)	Heart
(HGF/SF)	Hepatocyte Growth Factor-Scatter Factor

(HRP)	Horseradish Peroxidase
(kDa)	kilo Dalton
(Lam)	Laminin-1
(LTA)	Left Tibialis Anterior
(mpc)	muscle precursor cell
(MRF)	Myogenic Regulatory Factor
(MHC)	Myosin Heavy Chain
(Norm.)	Normalized
(OCT)	Ornithine Carbamoyltransferase
(PBS)	Phosphate Buffered Saline
(PAGE)	Polyacrylamide Gel Electrophoresis
(PCNA)	Proliferating Cell Nuclear Antigen
(RTA)	Right Tibialis Anterior
(SR)	Sarcoplasmic Reticulum
(SDS)	Sodium Dodecyl Sulfate
(SSC)	Standard Saline Citrate
(TNBT)	Tetranitroblue Tetrazolium
(T tubules)	Transverse tubules
(Rx)	Treatment
^{3}H-thymidine	Tritiated-thymidine

1. Introduction

Duchenne muscular dystrophy (DMD) is an X-linked, progressive disease caused by a mutation in the gene that codes for dystrophin (Hoffman et al., 1990). Mice with X-linked muscular dystrophy (*mdx*) experience an acute and extensive muscle fiber necrosis in limb muscles beginning at 3 weeks-of-age. However, unlike DMD muscle, *mdx* limb muscles show regeneration and recovery with little disability (Anderson et al., 1988; Bulfield et al., 1984; Torres and Duchen, 1987). The diaphragm of *mdx* mice exhibits more severe dystrophy as well as fibrosis like DMD (Stedman et al., 1991). The different phenotypes of muscles in the *mdx* mouse make it an ideal model for the study of disease severity, treatment success and repair.

Current treatments of DMD include two glucocorticoids, prednisone and deflazacort. Importantly, deflazacort has fewer side effects compared to prednisone (LoCascio et al., 1998; Angelini et al., 1994; Mesa et al., 1991). Both slow deterioration of muscle strength, ambulation and functional mobility suffered by DMD boys (Brooke et al., 1987; Khan, 1993). The exact mechanisms of glucocorticoid effects on DMD are unknown, although they do not work solely via anti-inflammatory mechanisms (Gray et al., 1991). In tissue culture studies, prednisone increases myoblast populations (Metzinger et al., 1994; Passaquin et al., 1993), and promotes myotube differentiation (Metzinger et al., 1994). However, while both prednisone and deflazacort promote fiber growth, deflazacort alone was found to promote repair in *mdx* limb muscle (Anderson et al., 1996). A close investigation of dystrophy and improved repair during deflazacort treatment is necessary to deduce the possible gene and cellular targets of the drug.

Ongoing work in our laboratory suggested that effects of deflazacort may be two-fold. Deflazacort may increase the proliferative rate of committed myogenic precursor cells (mpc) or their recruitment to the cell cycle. There are four myogenic regulatory factors (MRF) that are expressed in activated myoblasts before DNA replication (Grounds and Yablonka Reuveni, 1993) but not in quiescent satellite cells. Mpcs can be identified and their proliferation examined by investigating MRF expression during DNA synthesis (Anderson et al., 1998; McIntosh et al., 1998). Increases in mpc proliferation may underlie the increased formation of myotubes induced by deflazacort treatment.

Second, deflazacort may increase the expression of laminin, which could help stabilize a dystrophin-deficient membrane. Laminin, an extracellular matrix protein, is in direct contact with the dystrophin-glycoprotein complex (Ibraghimov-Beskrovnaya et al., 1992). Simo et al. (1992) demonstrated how treatment with a glucocorticoid could increase the expression of laminin in mesenchyme-derived cells. Changes in the abundance of laminin caused by changes in deflazacort may slow fiber degeneration or promote new fiber formation and stabilization.

These two ideas were investigated as part of an ongoing project to improve treatment of Duchenne muscular dystrophy.

2. Review of Literature

2.1 Overview of skeletal muscle structure, fiber typing and function

The contractile properties of skeletal muscle allow us to move and to carry out activities related to survival. Movements can occur over a short duration with quick contractions, over long periods with slow contractions, or through rapid rhythmic contractions. Three distinct types of muscles perform these types of contractions: skeletal, smooth and cardiac muscle, respectively. These muscle types are all mesodermally-derived, are elongated parallel to their axis of contraction, and contain a high concentration of mitochondria and contractile elements (myofilaments). The myofilaments of cardiac and skeletal muscle, actin, myosin and additional contractile-associated proteins, are arranged in a specific sarcomeric banding pattern that characterizes striated muscle (Huxley, 1963).

Skeletal muscle cells are elongated multinucleated cells typically known as muscle fibers or myofibers. The myofibers consists of cytoplasm (sarcoplasm), mitochondria and sarcoplasmic reticulum (SR), and are surrounded by a plasma membrane or sarcolemma. Each myofiber is cylindrical in shape and contains numerous elongated nuclei (often hundreds) that are generally localized to the periphery of the fiber with the non-contractile organelles. Skeletal muscles are surrounded by a dense collagenous connective tissue, called epimysium, which penetrates the muscle and separates it into fascicles. Each fascicle or group of fibers in turn is surrounded by perimysium, a looser connective tissue. And finally, each individual myofiber is further enveloped by fine reticular fibers, called

endomysium. The capillaries, lymphatics, and nerves pass through these connective tissue layers. The external or basal lamina directly surrounds each fiber.

Satellite cells are localized between the plasma membrane of myofibers and the basal lamina and are separated from myofibers by a very uniform and narrow cleft 15-25nm wide (White and Esser, 1989; reviewed by Bischoff, 1994). Satellite cells are found only in skeletal muscle, and are absent from cardiac and smooth muscle. Satellite cells are oval in shape, exhibit extended cytoplasmic processes and are often found in shallow depressions of the myofiber surface (depending on the fixation). Quiescent satellite cells have more heterochromatin than nuclei of myofibers, have a far greater nucleus-to-cytoplasm ratio than other cell types, and decline in numbers with age (Schultz and McCormick, 1994).

Following damage to the myofiber or through manipulations to collect satellite cells from muscle explants or for tissue culture, quiescent satellite cells are "activated" (defined as entry to the cell cycle) and subsequently express myogenic regulatory factors (MRFs; see section 2.7.3). Quiescent satellite cells can be identified by the expression of the c-met receptor, and activated satellite cells by the co-localization of both c-met and hepatocyte growth factor-scatter factor (HGF/SF; Tatsumi et al., 1998; reviewed by Anderson, 1998). Satellite cells may or may not divide after activation. If they do not divide, satellite cells regain quiescence and remain in the satellite position. However, if they do divide, the next generation of daughter cells, called myoblasts, proliferates 1-5 times and are thought mostly to become committed to the myogenic lineage. Eventually they differentiate and fuse to form replacement myofibers called myotubes. New myotubes have many nuclei within 4 days after an injury, at the peak of myotube

formation. Interestingly, the rate of new myoblast formation may be somewhat greater than the proliferative rate of typical satellite cells and therefore other locally-derived cells might also give rise to muscle precursors *in vivo*. It has been proposed that muscle regeneration may recruit cells from as far away as the bone marrow, or that bone marrow-derived multipotential stem cells are resident in muscle tissue (Ferrari et al., 1998).

Voluntary movements are initiated through innervation by efferent motor neurons. A motor unit consists of a motor neuron (with its nucleus located in the anterior gray horn of the spinal cord) and all the muscle fibers it innervates. Nerve impulses transmitted across the neuromuscular junction by the neurotransmitter acetylcholine, cause depolarization of the sarcolemma, which leads to muscle contraction. The wave of depolarization is distributed throughout the myofiber by transverse tubules (T tubules), which are invaginations of the sarcolemma. The T tubules are closely associated in triads with two terminal cisterns of the SR. During depolarization, the T tubules carry the impulse to the deeper layers of the myofiber, which causes release of calcium ions (Ca^{+2}) from the SR. Ca^{+2} will thereafter interact with the thin myofilament and actomyosin ATPase to cause the contraction of the sarcomeres. The arrangement of sarcomeres in parallel rows and synchronous contraction as a result of nerve impulses induces sarcomere shortening, fiber contraction, and force generation (Squire, 1997).

Myofibers can be divided into two basic types, type I (slow twitch) and type II (fast twitch) (reviewed by Staron, 1997). Apart from the motor neuron that innervates a fiber, it is the biochemical and isoform content of muscle-specific molecules such as myosin heavy chain (MHC) which together determine the fiber type. Type I fibers are characterized by a high activity of oxidative enzymes, the slow isoform of MHC, a high concentration of

mitochondria and a high lipid content. In addition, these fibers have a low content of glycogen and glycolytic enzymes, and are surrounded by many blood vessels. Together these features form slow-twitch, fatigue resistant fibers carrying out oxidative metabolism. Type II fibers are divided into three sub-types: type IIA, IIB and IIC. Type IIA fibers are fast-twitch, oxidative fibers. Type IIB fibers are fast contracting and glycolytic. Both type IIA and IIB fibers contain immunologically distinct fast MHCs. Type IIC fibers appear in transition between type IIA and IIB fibers and contain both types of fast MHCs. The function of the two fiber types also differs. Type I muscle fibers are best adapted for prolonged activity of low intensity, or endurance. Type II muscle fibers are best used for intense activity of short duration and fatigue more quickly than type I fibers.

2.2 Duchenne muscular dystrophy

Duchenne muscular dystrophy (DMD) is an X-linked progressive disease caused by a mutation in the gene that codes for dystrophin (Hoffman et al., 1990). Dystrophin is the largest known gene (2.4 megabases) in the human genome. It is located at Xp21.1 on the human X-chromosome, and is composed of 85 exons (Roberts et al., 1992). The gene product, which is missing, truncated, or abnormal in DMD patients, is a large rod-like cytoskeletal protein found along the inner surface of a muscle fiber sarcolemma. DMD is the most common of all known X-linked recessive disorders with a prevalence of approximately 1 in every 3500 male births (Brown and Lucy, 1993). The initial development of infants appears normal, but more than half fail to walk by 18 months. Greater than 90% of affected boys are wheel chair-bound by age 11 with 95% mortality by age twenty-one. Early signs of this disease include elevated creatine kinase (CK) isoform levels (see section 2.7.7), proximal limb muscle weakness, and

pseudohypertrophy of the calf muscles. Cardiac symptoms are almost universal and patients tend to have a lower I.Q. (one fifth of patients have mental handicaps or cognitive impairment). As well, in DMD muscle the very fast fibers (type IIB) disappear early and are either transformed or selectively degenerate. This results in relatively more type IIA fibers in DMD muscles than normal even before fiber loss becomes marked (Pedemonte et al., 1999).

2.3 Dystrophin, laminin and the dystrophin-glycoprotein complex

Dystrophin is part of a protein complex that bridges the inner cytoskeleton (F-actin), the sarcolemma, and the extracellular matrix (laminin). The absence of dystrophin and decreased abundance of associated proteins affects the integrity of the plasma membrane and its association with the extracellular matrix. During muscle contraction, the primary loss of dystrophin and secondary effects on associated proteins result in disruption of the membrane and subsequent degeneration of myofibers (reviewed by Petrof, 1998).

The dystrophin-glycoprotein complex is in direct association with laminin in the extracellular matrix and dystrophin beneath the plasma membrane. The dystrophin-glycoprotein complex is comprised of dystrophin-associated proteins (DAPs) and dystrophin-associated glycoproteins (DAGs). Proteins are given names according to their approximate molecular weights (25 and 59 DAPs and 156, 59, 50, 43 and 35 DAGs). Two further subcomplexes of dystroglycans and sarcoglycans have also been described. The dystroglycan complex is composed of α- and β-dystroglycans. Alpha-dystroglycan, an extracellular protein, binds to laminin in the basement membrane (Ibraghimov-

Beskrovnaya et al., 1992). Beta-dystroglycan, a transmembrane protein, binds to the cysteine-rich carboxyl(c)-terminal domains of dystrophin inside the cell (Ohlendieck, 1996). The sarcoglycan complex is composed of α-, β-, and γ-sarcoglycan (Lim and Campbell, 1998) which are all transmembrane glycoproteins. The precise nature of the association between the dystroglycan and sarcoglycan complexes remains unclear although they are absent from the plasma membrane of DMD patients and utrophin, a protein similar to dystrophin, appears in particular substitutions (Love et al., 1989). Therefore, dystrophin seems necessary for the proper formation of the complex since patients with DMD are only genetically deficient for the dystrophin protein.

Laminin, the most concentrated glycoprotein in the basement membrane (Martin, and Timpl, 1987) binds to the dystrophin-glycoprotein complex which in turn is linked to dystrophin. The laminin molecule has the shape of a cross and is formed as a heterotrimer of three subunits: a 400 kilo Dalton (kDa) heavy chain (α) and two 200kDa light chains (β and γ). The subunits are homologous but formed from different gene products. The α-subunit contains an additional 100kDa G-domain at the C-terminus, making it the heavy or dominant polypeptide of laminin. At the distal end of the α-chain through the last two globular repeats, laminin binds in a Ca^{2+}-dependent manner to α-dystroglycan, in the dystrophin complex (Gee et al., 1994; Ohlendieck, 1996). Dystroglycan exerts its influence on basement membrane assembly by binding soluble laminin and organizing it on the cell surface (Henry et al., 1998). Laminin assembly and secretion are controlled by the synthesis of the α-subunits, which has lead to the classification of laminins according to their α-subunits. The five isoforms of laminin are designated as α1, α2, α3, etc. The expression of the subunits is differentially regulated so that the subunits are

characteristically present only in certain tissues and at particular times of development (Wewer and Engvall, 1994). Laminin-1 (α1-β1-γ1), also referred to as classical laminin, is typically localized to the basement membrane of epithelial cells. The principal laminins present in basement membranes of mature muscle fibers are laminin-2 (α2-β1-γ1) and laminin-4 (α2-β2-γ1), which both contain the α2-chain and are collectively referred to as merosin or α2-laminin (Engvall and Wewer, 1995).

2.4 Treatment

While there are different treatments for DMD, all treatments ultimately attempt to increase function and strength, prevent progression within practical means and have minimal adverse effects. Such a treatment would, in addition, include supportive care to maintain mobility, prevent contractures, maintain ambulation, and use assistive braces for progressively weaker back and limb muscles. There are two additional approaches to treating DMD patients: genetic approaches and pharmacological therapies, each with its own specific targets. Genetic approaches attempt to introduce the missing dystrophin gene to dystrophin-deficient DMD patients either with dystrophin itself or with mini-dystrophin genes (reviewed by Partridge and Davies, 1995). Pharmacological agents, in contrast, attempt to make up for the absence of dystrophin by inhibiting or balancing some of the pathological consequences occurring in DMD patients.

In 1974, Drachman and his colleagues first raised the possibility of the beneficial effects of glucocorticoids in an uncontrolled trial of DMD patients. In contrast, Siegel et al. (1974) could not find any significant effect of glucocorticoids in a controlled study. There then followed a notable absence of formal trials until Brooke et al. published interesting results in a trial of prednisone in 1987 demonstrating that glucocorticoids

could slow the rate of decline of muscle strength. Current treatments of human DMD include two glucocorticoids: prednisone and deflazacort. The exact mechanisms of the glucocorticoid effects on DMD are unknown, although they do not work via anti-inflammatory and immunosuppressive mechanisms alone (Gray et al., 1991).

2.4.1 Prednisone treatment

Prednisone increases strength in DMD patients (Fenichel et al., 1991) and decreases cell death in human muscle cell cultures (Sklar and Brown, 1991). In humans, significant side effects of prednisone therapy include Cushingoid appearance, irritability, and decreased bone density (Khan, 1993; O'Connell et al., 1993). Because prednisone has clinically significant side effects, the therapeutic potential of prednisone is limited and its ability to truly benefit the overall function on a long term basis is questionable, despite being in general use to treat DMD patients.

2.4.2 Deflazacort treatment

Deflazacort has similar treatment effects as prednisone and increases muscle strength. Importantly however, it has fewer side effects than prednisone (Angelini et al., 1994; Mesa et al., 1991; Khan, 1993; LoCascio et al., 1998). Deflazacort is an oxazoline derivative of prednisone, and shares its immunomodulatory and anti-inflammatory properties, but is reported to have less serious inhibitory effects on specific leukocyte functions (Gray et al., 1991). Glucocorticoids affect the expression of many genes as receptors for glucocorticoids are present in the majority of cell nuclei, and may either positively or negatively promote gene transcription and/or translation (Schleimer, 1993).

2.5 Testing muscle strength

Clinical proof of successful therapy can be accomplished through testing muscle strength using functional performance scales (Brooke et al., 1983) or by observing progressive changes in histological preparations of biopsies. As biopsies are painful and destructive, tests of contractile function are the preferred means of assessing treatment effects. A protocol for the measurement of contractile force should be easy to use clinically, adaptable to the progression of the disease, inexpensive, and reproducible (Moxley, 1990). The Brookes Upper and Lower Extremity Grading Scale, a functional grade test, is a protocol that tests the effect of treatment on DMD. This test effectively reflects the course of illness and requires no equipment (Brooke et al., 1983; Lord et al., 1987). Reproducible lower extremity functional grade tests have been used by Mendell et al., (1989) and were shown to detect an increase in DMD muscle strength after a six-month trial of prednisone. More recent tests also include assessment of cardiorespiratory function in DMD patients (Hahn et al., 1997). However, this technique looks at cardiac muscle and not at skeletal muscle (except for the diaphragm), and therefore reflects only disease progression not limb muscle repair.

Animal models are important to medical research for the study of disease progression and new treatment improvements. The greater the similarity between an animal model and a human disease state, the more likely it is that an effective treatment in the animal model will be clinically beneficial in treating humans. However, in determining the treatment effects, functional tests should also model those used in a clinical situation. In animals, many different protocols are used to study contractile function. Testing endurance (prolonged activity of low intensity) selectively targets

fatigue-resistant type I fibers more than the fatiguable type II fibers. Alternatively, strength testing requires intense activity of short duration and thereby preferentially tests more of the greater force-generating, fatiguable type II fibers than the type I fibers.

Contractile function can be tested *in vitro* or *in vivo*. Bressler et al. (1983) adapted one particular protocol to determine whole muscle strength and speed of contraction obtained by stimulating a muscle (direct) or nerve (indirect). The muscle can be completely free of the limb (*in vitro*; e.g. Anderson et al., 1988; Ikeda and Mitsumoto, 1993). Alternatively the muscle under study can be mounted with the origin still fixed to the stabilized limb and the insertion tendon tied to a force transducer. This approach is useful as it maintains the intact blood and nerve supply (*in vivo*; e.g. Dangain and Vrobova, 1984). Accurate strength measurements of individual muscles can be obtained using both the *in vivo* and *in vitro* systems if they are optimally standardized. However, subsequent trials at a later time cannot be made because the animals must be sacrificed in order to record muscle strength. As a consequence, the effects of treatment on muscle strength over time cannot be determined unless groups of mice are killed at different treatment intervals. Such independent multiple trials would be susceptible to the influence of single time variation and in addition, are not practical to assess the longitudinal effects of treatment on one animal.

In vivo force tests can be performed as previously stated, obtaining contraction from a semi-isolated muscle stimulated either directly or indirectly. Alternatively, strength can be determined without manipulation as voluntary effort with no external stimuli. One such *in vivo* protocol to measure endurance in a non-manipulated animal is to measure the length of time an animal can remain afloat in a warmed (30°C) water-

filled chamber (Leeuwenburgh and Ji, 1995). However, due to the possibility of pneumonia from placing mice in water on a repeat basis, assessing the changes in endurance over time on the same animal are not possible with this technique.

Another *in vivo* protocol is the voluntary exercise treadmill commonly used to measure endurance. This can be used on one animal to measure changes in endurance throughout life. A limitation of this technique is first motivating the animal to run, although mice in captivity typically love the activity. In the *mdx* mouse (see section 2.6), the amount of voluntary running can be less than in normal control mice (C57BL/10)(Hayes and Williams, 1996; Dupont-Versteegdenn et al., 1994). This could be attributed to a lack of motivation due to pain caused by the degenerative effects of dystrophy rather than solely to muscle weakness. Limiting food intake to 1 session/day has been shown to improve the performance of voluntary running, although altering the nutritional status of the animals is not desirable (Russell et al., 1987). Finally, endurance training has mixed effects on *mdx* mice (see section 2.6). Hayes and Williams (1996) reported endurance training increased the number of oxidative fibers, reduced muscle fatigability, and improved force output. However, Podhorska-Okolow et al. (1998) reported spontaneous exercise-induced apoptosis of myofibers and satellite cells. In addition Brussee and Tardif (1997) reported that eccentric exercise (lengthening contraction) induces muscle damage by disrupting the sarcolemma. Without better studies of the exact effects of voluntary wheel running on dystrophic muscle and mice with dystrophy, investigation of treatment effects using running test protocols will be difficult to determine.

Meyer et al. (1979) developed an *in vivo* protocol to measure muscle strength over time. They used a calibrated force transducer from a commercial supplier (Chatillon, Largo, FL). Strength can be tested *in vivo* on the gauge by recording the forelimb grip strength (in grams) exerted on a bar by both forelimbs of a small animal (mouse or rat). This method fulfils the requirement to model human functional strength testing procedures. The equipment is inexpensive, the test is fast and efficient, there are minimal training effects if testing is limited, and importantly continuous data can be gathered from the same animal over time. Therefore this test protocol can be used to assess the benefits of treatment in animals and the results would be comparable to clinical muscle force tests in humans.

2.6 The *mdx* mouse model of DMD

There are several X-linked recessive animal models for DMD including the canine, feline, and *mdx* mouse models. Each of these can be used to study aspects of the neuromuscular and matrix abnormalities of the disease (reviewed by Nonaka, 1998). Canine muscular dystrophy is phenotypically similar to DMD and shows progressive weakness and death within 1 to 5 years. It is considered the most representative model of DMD. However, dogs are large and expensive to house, have a relatively long generation time, and are morally difficult to work with. Feline muscular dystrophy shows reduced muscle activity, stiff gait, and muscle hypertrophy similar to DMD. Little work is reported on the feline model primarily as the cats were euthanized prior to complete investigation.

The *mdx* mouse was discovered in 1984 in an animal breeding facility. *Mdx* mice experience an acute and extensive muscle fiber necrosis in limb muscles beginning at 3 weeks-of-age (Bulfield et al., 1984). The *mdx* mouse suffers from an X-linked muscular

dystrophy and has a point mutation (a substitution from cytidine to thymidine) at nucleotide pair 3185 in the dystrophin gene (Amalfitano and Chamberlain, 1996). By comparison, many mutations and deletions of variable size are seen in DMD patients. Initial interest in using *mdx* mice as a model for DMD declined, as *mdx* mouse dystrophy is not fatal like DMD. However, it was reported that *mdx* limb muscles show regeneration and recovery with little disability (Anderson et al., 1988; Bulfield et al., 1984; Torres and Duchen, 1987) so they could be used to model the regenerative phase of muscular dystrophy. Later studies showed that *mdx* mouse diaphragm muscle shows much more severe dystrophy than limb muscle, as well as fibrosis like that seen in DMD (Stedman et al., 1991). Therefore, the diaphragm of *mdx* mice can be studied to understand chronic muscle weakness, degeneration, and muscle treatment, while the limb muscle of *mdx* mice can be examined to determine the mechanisms underlying functional recovery. The different phenotypes of muscles in the *mdx* mouse make it an ideal model for the study of disease severity, repair, and the success of treatment protocols (Anderson et al., 1996).

2.7 Muscle regeneration

Regeneration after disease or muscle injury involves cellular infiltration, phagocytosis, sealing of damaged fiber ends, proliferation, fusion of muscle precursor cells (mpcs) into myotubes, and myotube growth (reviewed in Anderson, 1998). These processes and functional repair depend in addition on appropriate and adequate revascularization of the necrotic tissue area and reinnervation (if required) of new fibers or segments. Muscle membrane damage causes an elevation in intracellular calcium initiating necrosis and in turn, activation of complement and cell lysis (Engel and Biesecker, 1982). Regeneration is inhibited by necrotic tissue, and therefore phagocytosis

of necrotic tissue must precede effective muscle repair (Grounds, 1987). Phagocytosis also precedes revascularization (Roberts et al., 1989). However, the factors involved in attracting macrophages also stimulate revascularization (Robertson et al., 1993). Three hours after a crush injury, polymorphonuclear leukocytes are actively removing necrotic tissue, and at six hours macrophages out-number polymorphonuclear leukocytes and phagocytose the remaining necrotic tissue (Papadimitriou et al., 1990).

Revascularization is essential for successful muscle regeneration after injury. Without adequate new vessel formation, such as in large muscle grafts (see section 2.7.1.1), the central zone with low-oxygen tension does not regenerate completely and becomes fibrotic. Within such low oxygen environments, macrophages proliferate and secrete angiogenic factors. Since ischemia favors fibroblast growth, an inverse relationship may exist between good revascularization and fibroblast growth, resulting in areas of revascularization having low fibroblast content and vice versa (Storch and Talley, 1988).

In order to facilitate regeneration, the site of damage must also be isolated from the nearby undamaged sarcoplasm, segregating the surviving from the necrotic portions of the myofibers (Carpenter and Karpati, 1989). Necrotic lesions may be segmental in skeletal muscle because of the characteristic elongated multinuclear structure of myofibers. The sealing off process occurs early, 12 hours after crush injury (Robertson et al., 1990).

2.7.1 Experimental models of regeneration and treatment

2.7.1.1 Models of regeneration

The physical manifestations of a lack of dystrophin in both human DMD and *mdx* mice are muscle degeneration followed by regeneration. However, regenerating lesions are dispersed throughout the muscles and at any one time will present different stages of regeneration, from dying necrotic fibers to newly-regenerated centrally-nucleated fibers. In order to study regeneration systematically in a sequence from start to finish, the best models will initiate regeneration in a synchronized time course *in vivo* so that signals from non-muscle cells and the environment are maintained.

Different models for studying regeneration include denervation and devascularization (Zacharias and Anderson, 1991), minced muscle grafts, exposure to toxins (i.e. notexin, bupivacaine and marcaine) and the crush injury, which will all initiate the same sequence of regeneration but on different time scales and with variable success. Marcaine, a myotoxic anaesthetic, induces exogenous uptake of Ca^{+2} and increased necrosis of myofibers. However, not all fibers are affected, so while muscle damage occurs, the muscle is not uniformly damaged. This makes the regeneration less synchronous than in the crush injury model. Minced or whole muscle grafts (Lawson-Smith and McGeachie, 1997) are a model of well-synchronized regeneration. However, in the minced graft situation fiber reinnervation takes many weeks to complete because muscle grafts have no preexisting afferent or efferent nerves. The basal lamina is very disrupted in minced grafts unlike the situation in repair in the crush injury model. The crush injury model (McGeachie and Grounds 1987; McIntosh et al., 1994) is injury of a single muscle, which initiates a synchronized regenerative response. The mechanical

injury occurs when myofibers are directly crushed by closing a hemostat over the belly of the muscle. Importantly, vascularization and longitudinal orientation of the muscle *in vivo* are maintained with this model of regeneration. Regeneration after a crush can thereafter be characterized very well in a time-course manner for a particular animal. Regeneration after a crush injury varies between strains in age-matched mice. The SJL/J mouse demonstrates better regeneration than the BALB/c mouse (Mitchell et al., 1992). Repair in dystrophic *mdx* mice is more effective and advanced compared to repair in the normal parent strain (C57BL/10) (McIntosh et al., 1994; Pernitsky et al., 1996; McIntosh and Anderson, 1995). Mitchell et al. (1992) looked at two strains of mice, SLJ/J and BALB/c, and observed that both strains followed a similarly by ordered regenerative response to injury. However, the migration of inflammatory cells and mpcs to the site of regeneration after a crush injury was greater in SJL/J than in BALB/c mice.

The crush region (the central zone) of the tibialis anterior (TA) one day after injury contains a large population of necrotic myofibers and erythrocytes. In addition, distal and proximal to the central zone, the adjacent zones also contain necrotic tissue as well as mononuclear cells. By the end of the first day (24-30 hours after injury) replication of mpcs has begun (McGeachie and Grounds, 1987).

By day two post-injury, even more mononuclear cells are present in the adjacent zones and the central zone is much less necrotic due to ongoing phagocytosis. A greater proportion of mononuclear cells are proliferating (6-10% identified by autoradiography) than at day 1, and are apparent along the surface of the external lamina that is present around damaged fibers.

At three days after crush, there are numerous macrophages surrounding the central zone and there is no longer any necrotic muscle in the adjacent zones. Fusion of myoblasts into myotubes starts at 60-72 hours after injury. Young myotubes apparent at this time contain a maximum of 2-11 central nuclei (Robertson et al., 1990).

Between four and five days post-injury to the SJL/J mice, adjacent zones possess many newly-synthesized myotubes and the central zone consists primarily of mononuclear cells. However in regenerating muscle of the BALB/c mice four to five days post-injury, there are fewer myotubes and mononuclear cells, more connective tissue, and persistent necrotic tissue in the central zone. Mpcs are still actively proliferating 96 hours post-injury (McGeachie and Grounds, 1987).

By six to ten days after crush in the SJL/J mice, both the central and flanking adjacent zones are completely free of necrotic tissue and replaced with new myotubes and some connective tissue. By comparison, the BALB/c mice still have remnants of necrotic tissue, myotubes localized solely to the periphery of the central zone, and a greater amount of connective tissue with some calcification at this interval.

2.7.1.2 Treatment models

Gene therapy has a potential application to human disease and studies directed at restoring dystrophin or utrophin in *mdx* mice are used to characterize that potential. Myoblasts expressing either dystrophin or utrophin genes are transplanted into dystrophic muscle. In transgenic *mdx* mice expressing recombinant dystrophin or utrophin respectively, normal muscle morphology and function are restored (Winder, 1997; Inui et al., 1996). Reviewed by Gramolini and Jasmin (1998), utrophin is expressed along the sarcolemma in developing, regenerating and dystrophic muscles, and is localized to the

post-synaptic membrane of the neuromuscular junction in both normal and dystrophic muscle fibers. Because of a high sequence homology between dystrophin and utrophin, it was suggested that utrophin may functionally compensate for the lack of dystrophin (Love et al., 1989). A problem with the cellular approach to gene therapy has been primarily the low efficiency of myoblast transplantation due to cell death from immunological rejection (Miller et al., 1997). Vectors (viruses carrying genes) have been used as direct gene therapy or to transfect cells before transplantation. However due to the large size of native dystrophin, and the difficulty incorporating such large sequences into vectors, dystrophin mini-genes driven by muscle-specific regulatory elements, have been used with some success. Long-term side effects of transplantation and direct gene therapy approaches (cancer) have not been assessed, and before clinical trials are approved successful transplantation of the entire dystrophin gene, without an immune response must be accomplished (Floyd et al., 1998).

2.7.2 Muscle precursor cell proliferation

As indicated above (section 2.7.1.1) when skeletal muscle is damaged, quiescent satellite cells, the precursor cells of adult skeletal muscle, are activated and begin to proliferate (make DNA) by 24-30 hours after crush injury (Grounds and McGeachie, 1987). Often studies of repair use incorporation of tritiated (^{3}H)-thymidine into new DNA (and detection through autoradiography) as the marker of proliferation. Resulting myoblasts either divide again and fuse with one another to form young multinucleated muscle cells (myotubes), or fuse with the ends of damaged myofibers (reviewed by Anderson, 1998). The success of new muscle formation is related to the size of the injury. After a large injury, there is typically extensive disruption of muscle fibers and

replacement with fibrous and cellular connective tissue (McGeachie and Grounds, 1987). Satellite cells respond to injury within 4-8 hours as observed by the expression of myogenin and MyoD (MRFs, see section 2.7.3; Rantanen et al., 1995). Transcripts (mRNA) of marker genes such as c-fos and c-jun have also been observed as early as 3 hours post-trauma (Kami et al., 1995). Satellite cell activation *in vitro* and *in vivo* by hepatocyte growth factor-scatter factor (HGF/SF) apparently occurs via binding to the c-met receptor within 30 minutes after injury (Tatsumi et al., 1998).

The molecular mechanisms responsible for maintaining the quiescent state, initiating activation, and completing differentiation through many cycles of regeneration are not fully understood (Chambers and McDermott, 1996). The specific factor or factors initiating regeneration must be present even before the expression of MRFs, but to date are unknown. Influences from the host environment, inflammatory cells, growth factors and their receptors [particularly for fibroblast growth factor-2 (FGF-2)], and the extracellular matrix (Grounds, 1998) are each involved in maintaining the process, stimulating proliferation and remodeling muscle during repair. FGF-2, one suspected initiating factor, is in intact muscles sequestered and bound to heparin in the basal lamina, and is released upon injury (Kardami et al., 1988; Anderson et al., 1991). Growth factors specific for myogenic cells may also be released after injury possibly initiating activation (Chen and Quinn, 1992). However, this would only allow for activation of satellite cells near the site of injury and would not explain the activation of cells some distance away (McIntosh et al., 1994). Other signaling mechanisms may be physical strain and mechanical-chemical transduction (Anderson, in preparation).

A number of assays have been used to determine mpc proliferation while maintaining spatial orientation of cells in histological sections. Counting mitotic figures is a well-recognized, although crude method of assessing proliferation (Hall and Levison, 1990). More sophisticated methods, such as flow cytometry for DNA content of dispersed cells have been used for muscle precursor studies (Pernitsky and Anderson, 1996), but are more commonly used in immunological studies and do not maintain tissue integrity. ^{3}H-thymidine incorporation into new DNA and detection with scintillation counting or autoradiography of tissue sections is also commonly used (Anderson et al., 1987). More recent immunological methods using antibodies to cell-cycle-related antigens [i.e. proliferating cell nuclear antigen (PCNA) and Ki67] may be used with little expense or equipment. Currently, the most widely used antibody for detection of proliferation localizes bromodeoxyuridine (BrdU) a nucleotide analogue, which can be incorporated into new DNA.

2.7.3 Myogenic regulatory genes

Mpcs or myoblasts are derivatives of satellite cells and their proliferation. They can be identified by investigating their expression of muscle regulatory factors (MRF) in tissue sections (Grounds et al., 1992), based on the assumption that mpcs have been specified to the muscle lineage. When combined in tandem with studies of DNA synthesis (Anderson et al., 1998; McIntosh et al., 1998), the precise extent of proliferation of MRF-positive mpcs can be determined.

Muscle regulatory factors or MRFs are muscle-specific transcriptional regulators, which convert non-determined cells to myoblasts and myotubes (Weintraub et al., 1989). There are four MRFs, which are expressed in activated satellite cells before DNA

replication (Grounds et al., 1992). The MRFs are not expressed in quiescent satellite cells (Grounds et al., 1992; Cornelison and Wold, 1997). All four MRFs are basic helix-loop-helix (bHLH) proteins. The basic region is required for specific DNA binding, and the HLH sequences are required for the dimerization that precedes DNA binding (Davis et al., 1990). MRFs form heterodimers with other bHLH proteins such as E12 and E47. These in turn bind to E boxes (CAN-NTG) which are activation sequences. Once heterodimers bind to E boxes downstream muscle genes become transactivated (Kadesch, 1992, Pin et al., 1997).

The MRF genes act in two semi-redundant pairs, early and late in myogenesis (Rudnicki et al., 1993; Rudnicki and Jaenisch, 1995; Megeney and Rudnicki, 1995). Two of the MRFs (MyoD and myf5) act early and are required for determination (Yun and Wold, 1996; Cornelison and Wold, 1997). During muscle regeneration, MyoD is necessary for proliferation of early committed mpcs expressing myf5. However MyoD is not needed for proliferation of "pre-MyoD" or potential myoblasts (Megeney et al., 1996; Yablonka-Reuveni et al., 1999; McIntosh et al., 1998) or for progression through the myogenic process (Megeney et al., 1996). Two additional MRFs, myogenin and MRF4 act later and are differentiation factors (Weintraub, 1993). Myogenin mRNA expression *in vivo* starts at 6 hours and peaks at 48 hours with levels returning to baseline (zero) in regenerating muscle 8 days after a crush injury (Grounds et al., 1992). MyoD and myogenin proteins are present in satellite cells 4-8 hours after injury (Rantanen et al., 1995).

MRF mRNA can be localized and its distribution examined using *in situ* hybridization techniques. (Quantification of mRNA expression is best with Northern

blots; see section 4.4.2). *In situ* hybridization detects specific nucleic acid sequences in cells, tissues, and whole organisms. The principle of *in situ* hybridization is based on specific annealing of a labeled nucleic acid riboprobe to a complementary sequence of mRNA in fixed tissue, and the subsequent visualization of the probe. As opposed to standardized electophoretic separation methods (Northern blots), which provide information on the average nucleic acid content of a tissue homogenate, *in situ* hybridization can localize a specific target sequence within a mixed cell population such as that in a regenerating muscle. *In situ* hybridization allows for the analysis of relative MRF mRNA levels plus their spatial and temporal regulation and has proved to be a valuable tool in understanding gene expression and cell biology.

2.7.4 Laminin in regeneration

After an injury is sustained, regeneration leads to the creation of new fascicles of skeletal muscle and reorganization of surrounding supportive connective tissues. Laminin is an extracellular matrix protein that is in direct contact (linked) with the extracellular aspect of the dystrophin-glycoprotein complex (see section 2.3). The basal lamina as a whole (including laminin) functions as a scaffold, and is important both for proper regeneration and to minimize fibrosis (Grounds, 1991). Myoblasts produce and adhere to laminin (Kühl et al., 1982; 1986) which in turn can stimulate elongation, motility, proliferation and fusion of myoblasts in culture (Ocalan et al., 1988). Alpha2-laminin (α2-containing laminins, including laminin-2 and laminin-4), but not laminin-1 (containing the α1 chain but not the α2 chain of laminin), promotes myotube stability and prevents apoptosis, therefore increasing survival (Vachon et al., 1996). A complete absence of α2-laminin, as seen in the *dy/dy* mouse (Xu et al., 1994), or a mutation in the α2 chain of α2-laminin

(Vachon et al., 1997) results in fiber degeneration. As presented in section 2.3 a lack of dystrophin results in the loss of associated proteins including α2-laminin in *mdx* and DMD muscle. Therefore, in cultured myotubes derived from DMD patients or dystrophic *mdx* mice, laminin-α2-mediated adhesion is defective (Angoli et al., 1997). In addition, laminin expression has been observed to increase with dexamethasone, a glucocorticoid, in cocultures of embryonic gut epithelial cells and mesenchyme-derived cells. These reports suggest that if a treatment could increase the abundance of laminin, fiber degeneration (laminin-1) could be reduced or mpc proliferation, new fiber formation and stability (α2-laminin) may be increased. Laminin mRNA can be examined with Northern blot analysis or *in situ* hybridization on sections, while Western blot analysis can measure laminin protein. In this experiment α2-laminin mRNA (in laminin-2 and laminin-4) and laminin-1 protein were determined.

2.7.5 Differences between repair and muscle development

The field of skeletal muscle development in the mammalian embryo has exploded since the advent of transgenic mouse technology. Early work to predict and understand regeneration was presented in parallel with development. However, regeneration does not exactly recapitulate development.

Embryologicaly, most vertebrate muscles are derived from somites, blocks of mesoderm that form by segmentation of the lateral plate mesoderm (Keynes and Stern, 1988). Somites give rise to two distinct types of muscle. The myotomal muscles generate the axial and trunk musculature, and a migratory cell population colonizes regions of the developing limbs. In both instances, precursor proliferation, cell cycle arrest, and fusion

of individual myoblasts into multinucleated myotubes take place during muscle differentiation.

In development, myoblasts fuse and form elongated, multinucleated, cylindrical structures, called myotubes. The nuclei of myotubes are first located centrally but then are re-arranged to lie along the periphery of the maturing fiber. By comparison, nuclei stay in the centre of regenerated fibers. Myotubes form during development in a structured two-wave formation (Cho et al., 1994; Kelly and Zacks, 1969). During the first wave, both primary and secondary fibers form from fusion of myoblasts. Primary myotubes form from tendon to tendon (Haushka, 1994), and myoblasts remaining on the periphery of the primary myotubes proliferate. After some time, a second wave of fusion is initiated and secondary myotubes are formed. The new secondary myotubes form initially near the middle of a muscle fiber, in association with the neuromuscular junction, developing on primary myotubes (Duxson et al., 1989). Contractile myofilaments and cytoskeletal proteins in regeneration are expressed in mononuclear cells prior to fusion of myoblasts while some of those proteins are reportedly present only during or after fusion processes in development depending on their investigation by *in vivo* or *in vitro* assays (reviewed by Anderson, 1998).

Recent experimental progress has elucidated many of the molecular mechanisms that control myogenesis in the embryo (Montarras et al., 1991; Dias et al., 1994). Most of the advances in understanding development and regeneration have come from the identification and isolation of regulatory genes that are involved in controlling specific transcriptional events. Similar to regeneration, cells must commit to the muscle lineage (McLennan, 1994; Rudnicki et al., 1993; Arnold and Winter, 1998). Proliferation is an essential step in development since enough nuclear domains must be available for the huge

mass of muscle to develop. Differentiation is initiated by the expression of muscle-specific genes and followed by expression of genes for contractile and structural proteins. Both positive and negative inhibition, such as that from growth factors, hormones and MRFs will determine whether or not myoblasts will remain in the cell cycle or differentiate (Olson, 1992).

Bhagwati et al. (1996) and others have suggested that the pattern of expression of various MRFs in regenerating skeletal muscle differs from that of developing muscle in embryos. Importantly, of the four MRFs expressed during development, studies have shown a functional redundancy in early (MyoD and myf5) and late (myogenin and MRF4) MRFs. In development if either one of the early or late MRFs is absent, the other can compensate (reviewed by Anderson, 1998; Weintraub, 1993; Weintraub et al., 1991). In contrast, the absence of MyoD in regeneration cannot be compensated by myf5, and interferes with the proliferation of myoblasts (Megeney et al., 1996; Anderson et al., 1998).

2.7.6 Regeneration in dystrophy

Skeletal muscles of DMD patients undergo cycles of necrosis and regeneration, but the success of the repair phase decreases with age. Limb muscles become progressively weaker and fibers are replaced with small and large discrete lesions, accumulations of fat, and connective tissue. The regenerative capacity of DMD muscle is not sufficient to compensate for the continuous breakdown of muscle fibers characteristic of the disease process. In contrast to DMD muscle, *mdx* limb muscles show regeneration and recovery with little disability, and demonstrate better regeneration from a crush injury than the parent strain with normal muscle (C57BL/10) (Zacharias and Anderson, 1991; Anderson, 1998). The decline in regenerative capacity of DMD muscle is not due to a

fundamental difference in satellite cell morphology (Watkins and Cullen, 1986) or a reduced number of satellite cells (Watkins and Cullen, 1988). However, DMD muscle cells have a lower than normal capacity to divide in culture (Webster and Blau, 1990). It is believed that the continuous repetitive regeneration in diseases like DMD shortens the life span of satellite cells through a process that shortens the telomeres. This process limits the total number of cell cycles that one cell can undergo (Decary et al., 1996). Thus early in DMD, satellite cells can still proliferate and produce myoblasts, and this produces centrally-nucleated fibers that mark accumulated repair in DMD. However, due to the accelerated "cost" of divisions in aging DMD muscle, fewer satellite cells are capable of entering or completing the cell cycle. This results in rapid progression of muscle fiber loss and weakness.

2.7.7 Creatine kinase isoforms in regeneration

The primary source of energy for skeletal muscle is adenosine triphosphate (ATP). During muscle contraction, energy is produced by the break down of ATP, catalyzed by myosin-ATPase. Typically during relaxation, the level of ATP is recharged through the process of oxidative phosphorylation. ATP synthesis is catalyzed by calcium-ATPase. In instances of excessive exercise, ATP can also be supplied by using the high energy phosphate bond of phosphocreatine that is synthesized by the action of creatine kinase (CK). Phosphocreatine is an essential energy source for contraction, relaxation, and transport of substances within muscle cells. CK is the shortened term for the enzyme ATP:creatine N-phosphotransferase which catalyses the reversible transfer of a high energy bound phosphate groups between ATP and creatine phosphate. Through this

reaction, CK maintains the ATP levels for high energy requirements of skeletal muscle (reviewed by Bessman and Carpenter, 1985).

CK is a dimeric molecule consisting of two subunits: a mature M isoform (muscle type) and immature B isoform (brain type). These subunits are single peptide chains (360 amino acids, molecular weight 41000 daltons) with an active centre capable of enzymatic activity. Together they form dimers MM, MB, or BB. The mature M subunit is the most common form present in mature skeletal muscle (Yamashita & Yoshioka, 1991), but the immature B subunit is also expressed in skeletal muscle and is a marker for skeletal myogenesis (Lough and Bischoff, 1977). CK isozyme gene expression is regulated by myogenic factors like MyoD (Lyons et al., 1991). Interestingly, developing muscle exhibits a characteristic pattern of expression of CK isoforms that progresses from immature BB CK expression to more mature MB and MM expression through development (Ziter, 1974). The differences in isoform expression and abundance of the enzyme make CK an ideal index for monitoring energy metabolism during muscle regeneration (Morris, 1978). Bischoff and Heintz (1994) were first to apply this to studies of the sequence of isoform expression over time after muscle injury. Muscles were injured by freezing to kill fibers, and then regenerating muscles were examined at various times after injury for total CK activity and isozyme levels. Isozymes were separated electrophoreitically on a zymogram agarose gel.

The MB and BB isozymes of CK leak into the serum from muscle of patients with various neuromuscular disorders including DMD, due to muscle fiber breakdown as first described by Ebashi et al. (1959). In DMD, the pattern of CK isozymes detected in affected muscle tissue appears similar to that seen in fetal muscle (Kuby et al., 1977).

Information regarding the stage and the success of regeneration of muscle can be gathered from a differential analysis of CK isozymes (Bischoff and Heintz, 1994). Since the shift from immature (BB) to more mature (MM) isozymes occurs during the 2-4 day recovery period after injury, the present experiments were designed to sample regenerating muscle at exactly this interval for CK isozymes, laminin, and MRF+ mpc proliferation during deflazacort treatment.

2.8 Treatments that modulate repair in dystrophic animal muscles

Prednisone increases the strength and endurance of *mdx* mice (Hudecki et al., 1993). In cultured cells prednisone promotes myogenesis (Passaquin et al., 1993) and fusion of myoblasts into myotubes (Metzinger et al., 1994). *In vivo* studies of regeneration by Anderson et al. (1996) showed that treatment of *mdx* mice with deflazacort or prednisone increased the diameter of muscle fibers, but that only deflazacort increased the central nucleation index used to study muscle regeneration. In regenerating muscle, the fusion of mpc and myotube growth were also increased by deflazacort. In addition, with deflazacort treatment the diaphragm muscle was much less inflamed and the diameter of fibers greater than with placebo injection. Since scientific improvement of therapy requires a thorough understanding of treatment mechanisms, a close investigation of dystrophy and improved repair during deflazacort treatment is needed to deduce the possible gene and cellular targets of the drug.

3. Hypothesis and Objectives

The long term goal of this study is to determine the mechanisms underlying the beneficial effects of deflazacort treatment in DMD. Deflazacort is currently used in clinical trials for human DMD; however, very few *in vivo* studies of mpc proliferation, fusion, gene expression or myofiber growth and development can be performed on humans. Thus the detailed study of the *mdx* mouse may reveal clinically relevant and important positive and negative drug treatment effects.

3.1 Hypothesis

Deflazacort treatment causes a positive change in the proliferation of MRF-positive myogenic precursors, and the expression of laminin, and these effects relate to increased strength in *mdx* dystrophic muscle during treatment.

3.2 Specific objectives

1. Test the functional strength of muscle *in vivo* before, during, and after deflazacort treatment.
2. Examine MRF+ mpc proliferation using autoradiography and *in situ* hybridization in muscles regenerating with and without deflazacort treatment.
3. Study the effects of deflazacort treatment on the level of expression of laminin in regenerating muscles using Northern and Western blots, and using creatine kinase activity to standardize expression to new myotube formation.

4. Materials and Methods

An *in vivo* study was carried out to determine muscle cell proliferation, gene expression and muscle strength in *mdx* mice with and without deflazacort treatment.

4.1 Animals and treatment protocols

The mice used in all experiments, *mdx* and C57BL/10 mice, were housed at the Central Animal Care facility at the University of Manitoba, in accordance to the guidelines of the Canadian Council on Animal Care. In addition, the mice were free of mouse hepatitis virus and procedures were approved by the University of Manitoba Animal Care Committee (Ref # 97-115).

Twenty-seven *mdx* mice were used and randomly assigned to one of two possible treatments and equal numbers of males and females were assigned to each group. Thirteen *mdx* mice received deflazacort treatment and 14 received placebo treatment. Using a double-blinded protocol, a dose of 1.25mg/kg deflazacort (Marion Merrell Dow Inc., Laval, PQ) or equal volume of placebo (Methocel, CIBA Vision, Mississauga, ON) was injected subcutaneously daily from 3 to 7 weeks-of-age. After 4 weeks of treatment, mice were anesthetized (1:1 ketamine-xylazine) and the right tibialis anterior (RTA) muscle was isolated and crush-injured (McIntosh et al., 1994), as described in section 4.3.1. In addition, a repeat experiment was performed in which 10 *mdx* mice were randomly divided into two treatment groups, deflazacort (n=5) and placebo (n=5) and treated daily for two weeks.

4.2 Muscle strength tests

Forelimb grip strength was measured with a Chatillon gauge according to modifications of a procedure outlined by Meyer et al. (1979). The gauge was mounted on an apparatus constructed from 9mm thick plexi-glass. The base was 51cm long and 25cm wide with a 30cm x 10cm hemisphere platform resting on a 6cm high stand (Figure 1A). The push-pull gauge (Chatillon, Model DFM-2.0 kg) was positioned at one end of the platform on an adjustable stand, positioned at a height of 10cm above the platform and 45° to the horizontal. The strain gauge had a bar attached for animals to grip. The bar was a 3.2cm equilateral triangle made of a 3mm diameter aluminum rod. The Chatillon gauge extension arm was attached to the triangular grip bar. Both were aligned to be parallel to the direction of pull (45° above horizontal), to ensure that the force from experimenter through the mouse to the bar were vectors in a straight line. Preliminary experiments indicated that a bar was the most effective object for a mouse to grip securely in order to optimize strength measurements. In a pilot test, use of the bar produced 44% higher strength measurements than a screen mesh. As well a bar thicker than 3mm was too large for mice to grip well.

Grip strength was assessed by holding mice by the tail and lowering them towards the bar until their forelimbs were securely grasping the bar. They were held as close to their body (at the base of the tail) as possible without their hind limbs touching the experimenter's hand or bar. Once the mouse established a strong grip, verified by rocking the animal back and forth, the mouse was pulled smoothly in a direction parallel and away from the gauge at a 45° angle to the horizontal. The peak tension (strain) generated by the mouse was recorded on the Chatillon gauge in grams. Each test consisted of four trials (of

three pulls per trial) administered over two days. Trials lasted no longer than one minute, and re-trials were attempted after sufficient rest, approximately 20 minutes. In preliminary studies, measurements of the peak strength from individual animals were consistent (±7%) and reliable within (±4%) and between (±6.5%) investigators.

Mice were tested for muscle strength before and during treatment. The peak force a mouse could pull with both forelimbs on the gauge was determined and recorded. Strength tests were done twice prior to treatment (-2 and -1 days), and then at day 9-10, 19-20, and 26-27 of treatment with deflazacort or placebo. In this case the peak strength (maximum of all 12 pulls over 2 days) was collected for each animal and the mean peak strength was plotted (normalized to body weight) as a function of treatment time (days). In a repeat experiment, another group of animals (deflazacort n=5; placebo n=5) were treated daily from 3 to 5 weeks-of-age. Strength tests were administered during treatment, and were administered weekly for six weeks after treatment to follow the post-treatment effect of deflazacort. In this case the mean al all 12 trials was calculated for each mouse and the average mean strength (normalized to body weight) was determined for each group and plotted as a function of treatment time (in days). Two-way analysis of variance (ANOVA) with replication (time) was used to compare treatment groups over time. Duncan's post hoc multiple range test was used to determine differences between pairs of means ($p \leq 0.05$).

4.3 Crush surgery and tissue collection

4.3.1 Crush surgery

A crush injury was used to initiate a synchronous regenerative process using the technique of McGeachie and Grounds (1987) modified according to McIntosh et al. (1994). The *mdx* mice were anesthetized using a 1:1 ratio of 100mg/mL ketamine (final

concentration = 1.5mg/mL) and 20mg/mL xylazine (final concentration = 0.3mg/mL) administered intra-peritoneally at 1.5μL/g body weight. Thereafter, the hair covering the lower anteriolateral aspect of the right leg was trimmed, and the skin was scrubbed with iodine soap, rinsed clean, and dried. An incision was made on a proximal-to-distal orientation, from just below the knee to the lateral aspect of the ankle. The investing compartmental fascia was cut and removed by blunt dissection from the belly of the right tibialis anterior muscle (RTA) beneath. The fascia around the RTA was separated from underlying muscles. At the mid-belly of the RTA (1cm proximal to the calcaneus), an open hemostat was placed around the RTA and then closed (to the first "click") for 5 seconds. The hemostat was then opened and carefully, removed and the crush region marked by placing two sutures (one above and one below, separated by a total distance of 3 times the length of the crush). The skin was then sutured closed with silk (5-0). The contralateral left tibialis anterior (LTA) of each mouse did not have a crush and served as a control.

4.3.2 Labeling proliferating cells

After 4 days recovery from the crush injury, intraperitoneal injections of 1.0mL/100g body weight of bromodeoxyuridine (BrdU, Amersham) and 2μCu/mg body weight of ^{3}H-thymidine were given approximately 24 h and 2 h prior to sacrifice, respectively. When exposed to these agents as single pulses, cells that were synthesizing DNA were labeled by the uptake of a non-radioisotopically-labeled nucleotide analogue, BrdU or a radioisotopically-labeled nucleotide. This enabled the study of cell proliferation using immunostaining or autoradiography, respectively. A segment of the small intestine (jejunum) was also collected as a positive control, since gut epithelial cells

divide continuously. Therefore, cells from the gut would be labeled by both ^{3}H-thymidine and BrdU absorbed from the peritoneal cavity into the blood stream. Sections were examined for BrdU uptake in another study.

Animals were euthanized by cervical dislocation under ether anesthesia and skin removed by eversion.

4.3.3 Tissue collection and sectioning

After skinning the animal, the LTA and RTA were dissected from the limbs and cut in three equal parts along the longitudinal plane. The central part of the muscle was put immediately in ornithine carbamoyltransferase (OCT; Sakura) and frozen by immersion in isopentane (-50°C) for later sectioning. The medial part of the LTA and RTA were placed in eppendorf tubes and frozen in liquid nitrogen for the later extraction of RNA or protein for Northern or Western blots, respectively. Importantly, before the medial part of the RTA was frozen, muscles were cut at the sutures above and below the centre of the crush. This isolated the synchronously-regenerating area of the RTA sample. The lateral thirds of the RTA and LTA were collected and pooled from the groups for immediate assay of CK activity.

The diaphragm was also collected. It was isolated from the abdominal side by first retracting the liver and intestines into the lower abdomen, and cutting the esophagus and the attached ligaments. Next, while holding the diaphragm by its central tendon from the abdominal aspect, the diaphragm was removed from the thorax as a unit by cutting along costal margins around its circumference. The thinner anterior portion was separated from the dorsal segment (crura) cut into three segments, and placed in eppendorf tubes to be frozen for later Northern and Western blot assays, in addition to immediate CK assay.

The crural section was then prepared for frozen sectioning by embedding in OCT and freezing.

Finally, the heart was exposed by opening the thoracic cavity by a longitudinal incision through the sternum. The heart was removed, placed on a clean surface (anterior surface face up) and cut in the sagittal and coronal planes into quarters. The two posterior quarters were placed in eppendorf tubes and frozen in liquid nitrogen. One of the two anterior quarters was embedded in OCT for frozen sections and the other anterior quarter was used immediately for CK analysis.

In a preliminary study to determine whether strength testing affected the extent of fiber damage in dystrophic muscles, forearm muscles were collected and prepared for frozen sections. Anterior and posterior muscles of the right forearm were dissected from 5 mice. Twenty-four hours prior to collection of tissue, three of the five mice received strength tests, 3 trials (of one minute) in the morning and 3 trials in the afternoon, while two mice were not tested. At the end of the test day, 20 hours prior to sacrifice, 1ml/20g body weight Evans Blue (Sigma Chemicals, St. Louis) was injected subcutaneously. The dye is excluded from intact muscle fibers but penetrates broken fiber membranes. Muscle fibers infused with dye fluoresced red (Brussee et al., 1997). Sections were photographed on an Olympus BHT-2 RFCA light microscope, using an Olympus C-35AD-4 camera and 400 ASA black and white film (see section 4.9). There was no observable or statistical difference in the area of fluorescent muscle between mice which had undergone strength testing, and mice which had not (Figure 1B). Therefore the occasional strength tests performed to determine strength in the deflazacort treatment experiment had no apparent effect on the integrity of muscle fibers.

All tissues embedded in OCT were sectioned longitudinally and/or in cross-section (7μm thickness) and collected onto silanated slides. Sections were stored at -20°C until required.

4.4 Creatine kinase isoform expression

4.4.1 Activity assay

CK was assayed using a protocol developed by Bischoff and Heintz (1994). Fresh samples of RTA, LTA, diaphragm, and heart muscle were collected, weighed and homogenized on ice in 2mL of 50mM Tris-HCL buffer (pH 7.5), with 1mM dithiothreitol and 1mM phenylmethyl sulfonyl fluoride using a homogenizing microprobe (Kinematica AG; polytron 1200). The homogenate was centrifuged twice at 2000g for 10 minutes and the pellet re-homogenized in 5mL of the same buffer. The supernatant was dialyzed overnight against a Tris buffer using a regenerated cellulose tubular membrane (Fisherbrand, Fisher Scientific, ON) and stored at -70°C. Total CK activity was assessed using a Creatine Kinase kit (Sigma procedure 661-PB) to determine the phosphorylation of creatine by ATP. This was followed by hydrolysis of the phosphocreatine to yield inorganic phosphorus, which was then measured at 690nm on a spectrophotometer. Total CK activity was determined for each sample and sample activities were equalized by dilution to 2μg phosphate per μL.

4.4.2 Separation and quantification of isoforms

After addition of glycerol, the different CK isoenzymes (BB, MB, and MM) were separated by electrophoresis in a thick 1% agarose gel. The samples were loaded in the gel (5μL/lane) and equilibrated with a Sigma creatine phosphokinase equilibration reagent according to a Sigma Diagnostics Creatine Kinase-MB reagent kit (Sigma

procedure 49-UV). The gels were run at 75V for 2 hours at 4°C and incubated in a solution containing the necessary substrates and indicator enzymes (Sigma) to form a purple-coloured insoluble precipitate, tetranitroblue tetrazolium (TNBT)-formazan, which localizes to the bands of CK activity. Gels were finally rinsed in water.

CK isoform levels were determined by scanning gels that showed separated BB, MB and MM CK isoforms (MCID 3.0; St Catherines, ON) and the optical density obtained for each isoform (minus background). Isoform levels (expressed in optical density units) were compared between groups using Chi-squared statistics. As well, the proportionate level of MM isoform activity over total CK activity was used to normalize expression of laminin mRNA and protein from Northern and Western analyses, respectively in an attempt to find changes in laminin expression relative to muscle content in regenerating regions.

4.5 mRNA expression

In situ hybridization and Northern analysis were used to identify α2-laminin expression with 3kb α2-chain specific riboprobes (α2-laminin cDNA kindly given by Dr. Eva Engvall). *In situ* hybridization on sections was used to identify myogenic cells using riboprobes for MyoD (Davis et al., 1987) and myogenin (Wright et al., 1989). All riboprobes were labeled by run-off transcription exactly as reported (Garrett and Anderson, 1995) with digoxigenin-conjugated uridine triphosphate nucleotides (Boehringer Mannheim, Laval, PQ). Digoxigenin (DIG)-labeled riboprobes were able to detect 7.5 pg of myogenin- and MyoD-homologous RNA by blot hybridization. The sensitivity of the α2-laminin probe was less than 0.1ng of RNA.

4.5.1 *In situ* hybridization

Sections were processed for *in situ* hybridization of α2-laminin, MyoD and myogenin mRNA according to a method described by Garrett and Anderson (1995). Frozen sections on slides were warmed to room temperature, fixed with 4% paraformaldehyde in phosphate buffered saline (PBS) for 15 minutes, and washed 2x in PBS for 10 minutes. Control slides received treatment with either DNase (50μL/mL in 40mM Tris buffer; pH 7.5, with 6mM $MgCl_2$) or RNase (50μg/mL in 0.01M sodium acetate; pH 5.2, 0.1M Tris buffer; pH 7.4) for 15 minutes at 37°C under coverslips. After treatment, coverslips were removed and sections were washed with millipore water and diethyl pyrocarbonate (DEPC) water.

Prior to use on slides, the hybridization buffer was heated to 95°C for 10 minutes and quenched on ice. Sections were pretreated for 1 hour at 42°C with 20μL hybridization buffer under a coverslip and washed with DEPC water. Digoxigenin-labeled probes (against MyoD, myogenin or α2-laminin) together with hybridization buffer, were heated to 95°C for 10 minutes and then quenched on ice. Slides were then hybridized with 20μL of probe in hybridization buffer under coverslips sealed with rubber cement. Hybridization was carried out overnight at 42°C in a humid chamber.

Coverslips were removed the following morning and slides were washed twice with double concentration standard saline citrate (SSC), 0.1% sodium dodecyl sulfate (SDS) in DEPC water for 15 minutes each, followed by further washings twice with 0.1x SSC, 0.1% SDS at 37°C for 15 minutes each. Probe detection involved rinsing slides twice with DIG Buffer 1 (Boehringer Mannheim, Laval, PQ), followed by blocking with DIG Buffer 2 for 60 minutes and then rinsing again with DIG Buffer 1 for one minute. To

detect the hybridized probes, an alkaline phosphatase-conjugated antibody against digoxigenin (α-DIG-AP) (Boehringer Mannheim, Laval, PQ) was diluted 1:500 in DIG Buffer 2, placed on slides covered under coverslips, and incubated overnight at 4°C. Other negative controls included the omission of the probe, omission of antibody against digoxigenin (α-DIG-AP) and omission of both the probe and α-DIG-AP. The following morning, slides were washed twice for 15 minutes with DIG Buffer 1 with agitation and equilibrated in DIG Buffer 3. A colour solution (9.0μL nitroblue tetrazolium salt [final concentration = 0.35 mg/mL], 7.0 μL 5-bromo-4-chloro-3-indolylphosphate [final concentration = 0.175 mg/mL], and 20 μL 24 mg/mL levamisole in 2 mL Buffer 3) was applied to the slides and allowed to develop in the dark (solution is light sensitive). At the appearance of a colour precipitate, occurring typically within 14 hours at room temperature, slides were washed with DIG Buffer 4 to stop the colour reaction. Finally, the slides were briefly stained with 2 quick dips in hematoxylin and left in running water for 5 minutes to wash away excess blue. Sections could not be exposed to acid alcohol or dehydrating alcohol because those solutions would remove the colour precipitate. Sections were air dried overnight, prepared for autoradiography (Anderson et al., 1998) (see section 4.5) and mounted in Aquamount (Lipshaw Immunon, Pittsburgh).

Alpha2-laminin mRNA expression and localization in the regenerating region of muscles were observed and photographed on a BHT-2 Olympus microscope. The distribution of signal in mononuclear cells, myotubes and myofibers was compared between deflazacort- and placebo-treated groups. See section 4.7 for the assessment of mpc proliferation.

4.5.2 Northern analysis

4.5.2.1 RNA isolation

Total RNA was isolated from the frozen *mdx* muscle samples of RTA, LTA, diaphragm, and heart with a phenol/chloroform solution according to Chomczynski and Sacchi (1987). RNA isolated from the nucleus or cytoplasm by such direct cell lysis is known as steady state RNA, representing the total RNA in the cell. The experiments to assess relative changes in mRNA and protein expression induced by deflazacort treatment were all made from muscles collected from the same set of mice, which was different from that reported by Anderson et al. (1996).

The tissue weight was recorded, samples in each group were pooled, and the tissues were homogenized. The total RNA was extracted by adding a phenol/chloroform solution and placing the samples on ice for 10 minutes. Samples were centrifuged at 10,000 g for 10 minutes. The supernatant was removed and added to 600μL isopropanol and left to precipitate overnight at -20°C. Samples were again centrifuged at 10,000 g for 20 minutes, the pellet was removed and dissolved in 180μL solution D and 180μL isopropanol and left overnight at -20°C. Samples were centrifuged at 13,000 g for 10 minutes, supernatant removed, pellets dried, and re-suspended at 65°C in 50μL 0.5% SDS. Finally, concentrations of RNA samples of known volume were determined using a spectrophotometer (Spectronic Genesys 5) at an absorbance of 260nm and 280nm, taking in consideration the known absorbance of 1μL of RNA.

4.5.2.2 Gel electrophoresis and Northern blotting

The RNA samples and the 3kb probe for the α2-chain (used as a size marker and positive control) were prepared for Northern analysis according to Boehringer Mannheim DIG system user's guide for filter hybridization (1995) and Rueger et al. (1996). All samples were denatured (50% formamide, 10% MOPS, 17.5% formaldehyde, 10% Glycerol, 0.025% Bromophen Blue, .5% ethidium bromide) for 20 minutes at 65°C and quenched on ice for 10 minutes. Following this, the samples (approximately 10μg/well) were run on a 1.2% agarose/formaldehyde gel for 4.5 hours at 25V. Before running the gel at 25V however, the samples were run at 50V for approximately 5 minutes with just enough MOPS to conduct a current but not to fill the wells. This procedure ensured that samples had completely entered the gel and were not washed out of the wells by filling with buffer. After running the gel, RNA was transferred overnight to a nylon membrane (Boehringer Mannheim, Laval, PQ) by capillary action with SSC buffer. The membrane was baked for 30 minutes at 120°C and exposed to UV light for 1 minute to immobilize the RNA. Next the ethidium bromide-stained RNA bands on the membrane were visualized using a UV transilluminator to verify the integrity of the samples. Membranes, now containing fixed RNA, were pre-hybridized for 2 hours at 68°C (in 50% formamide, 5x SSC, 0.1% N-lauroyl sarcosine, 0.02% SDS, and 2% Boehringer blocking solution), and hybridized with DIG-labeled riboprobes (100ng/mL) overnight at 68°C. After hybridization, membranes were washed twice in 2x SSC containing 0.1% SDS for 5 minutes at room temperature and twice in 0.1x SSC containing 0.1% SDS at 68°C for 15 minutes.

The hybridized DIG-labeled probes were identified using immunological detection. The membrane was blocked for 30 minutes with Buffer 2. Anti-digoxigenin-AP was diluted 1:10000, centrifuged at 13000 rpm for 1 minute, and placed on the membrane (in an incubation bag) for a total incubation period of 30 minutes at room temperature. The membrane was washed with washing buffer twice for 15 minutes, equilibrated with Buffer 3 (without $MgCl_2$) for 2 minutes, and a chemiluminescence substrate for alkaline phosphatase (CSPD) (diluted 1:100 with Buffer 3, without $MgCl_2$) for 5 minutes. Following this, the membrane was placed between two transparent acetate sheets in an air-tight bag for 15 minutes at 37°C. Finally, bands on the membrane were visualized on X-ray film developed after exposure for approximately 1 hour.

4.5.2.3 Quantification of mRNA expression

Blots from Northern analysis of α2-laminin mRNA were scanned (MCID 3.0; St Catherines, ON) and the relative optical density (minus background) measured. The adjusted optical density of blots was then normalized to the RNA loaded on each lane of the gel, and secondly to the weight of the muscle sample, therefore minimizing any discrepancy differences in the size of the animal would have on the amount of mRNA. In addition, CK isoform levels (see section 4.8.3) were used to normalize mRNA expression of α2-laminin gathered from Northern blots. The relative change in the expression of α2-laminin mRNA after treatment was given as a ratio of deflazacort to placebo for each tissue.

4.6 Autoradiography

DNA synthesis was detected from the incorporation of a thymidine analogue (^{3}H-thymidine) over a short exposure time during the S phase of the cell cycle. Following the

in situ hybridization protocol, incorporated radioisotope was detected using autoradiography (RAG; Ilford K5 emulsion) described by Wilkinson (1992). Autoradiography involved three steps: first, tissue sections on slides were dipped into liquid emulsion and allowed to dry. Second, the slides were exposed at 4°C for an appropriate time (7 weeks) as determined with the positive control sections. Finally, the exposed silver grains were developed, fixed and dried.

4.7 Measuring proliferation by muscle precursor cells

Sections prepared for both *in situ* hybridization of MRFs and autoradiography for DNA synthesis were viewed at 400X magnification. Cell counts were performed for MRF+, RAG+, or MRF+/RAG+ in the regenerating muscles moving progressively medial to lateral, proximal to distal within the region adjacent to the crush injury. Up to 300 cells in the regenerating regions of the RTA were counted. The proportion of MRF+/RAG+ cells were compared between deflazacort- and placebo-treated groups for MyoD+ (committed) and myogenin+ (differentiated) mpcs. The distributions (frequency counts) were compared between deflazacort- and placebo-treated groups using Chi-squared statistics ($p \leq 0.01$). Note that the studies of expression for mRNA and protein on sections were made using slides prepared from the earlier work on regeneration reported in part by Anderson et al. (1996).

4.8 Protein expression

4.8.1 Western analysis

4.8.1.1 Protein

Total protein was isolated from samples of *mdx* RTA, LTA, diaphragm, and heart muscles. Pooled samples were weighed and then homogenized in 2 mL of 2.5 M Tris-

HCl buffer (pH 7.2) for approximately 2 minutes. Homogenized samples were centrifuged at 0°C for 15 minutes at 6000 rpm. Soluble protein was removed by collecting the supernatant and freezing it at -70°C for 20 minutes. The supernatant was lyophilized over night. Samples were resuspended in water and protein concentration was determined by Lowry assay using a spectrophotometer (595nm, Spectronic Genesys 5). Bovine serum albumin (BSA) Fraction V (Sigma Chemicals, St. Louis) at a known concentration was used as a relative protein standard for all assays.

4.8.1.2 Gel electrophoresis and Western blotting

Muscle samples, high molecular weight markers (Bio-Rad), and a positive control sample of laminin-1 (L2020, Sigma Chemicals, St. Louis) were prepared for sodium dodecyl sulfate (SDS) polyacrylamide gel electrophoresis (PAGE) by diluting all samples to similar concentration with SDS-containing loading buffer according to Bio-Rad manufacturers instructions (catalog number 170-3935). The anionic detergent, SDS binds to the hydrophobic regions of proteins and separates them into component denatured polypeptides that bear a negative charge and are easily separated by electrophoresis. Equal protein aliquots (5µg/well) were boiled for 5 minutes, quenched on ice, and loaded into the wells of 7.5% separating, 4% stacking 8cm x 10cm mini-gels. The proteins were fractionated by running gels at constant voltage (200V) for 45 minutes at room temperature in running buffer. The gels were then immersed in transfer buffer. Nitrocellulose membrane (Bio-Rad, 0.45µm) was cut to size, pre-soaked in methanol for 15 seconds, and equilibrated in transfer buffer for at least 15 minutes. The membrane and gel were placed between two 3 M chromatography papers pre-wet in transfer buffer, and proteins were transferred (blotted) at 4°C for 1 hour at 100V. To confirm that transfer

was complete, the gels were observed for any bands after they were stained after blotting with Coomassie blue [20% (v/v) methanol, 7.5% acetic acid, 0.04% (w/v) Coomassie brilliant blue] for 1 hour with gentle agitation, and destained in 20% (v/v) methanol and 7.5% (v/v) acetic acid at room temperature.

The membrane with bound proteins was blocked with blocking reagent for 30 minutes, rinsed 3 times in 1x PBS for 1 minute, and immunostained for 2 hours (with agitation at room temperature) with a primary polyclonal anti-laminin-1 antibody (L9393, diluted 1:100; Sigma Chemicals, St. Louis). The polyclonal anti-laminin-1 antibody was raised commercially in rabbit using L2020 laminin-1 (Sigma Chemicals, St. Louis) which was purified from the basement membrane of Englebreth-Holm-Swarm mouse sarcoma tissue. The same laminin (L2020) was used as a positive control in Western blotting. Membranes were then washed 3 times in 1x PBS for 15 minutes and incubated with the secondary antibody [donkey anti-rabbit Ig, conjugated with horseradish peroxidase (HRP) diluted 1:100; Amersham] for 1 hour at room temperature with agitation. Membranes were washed 3 times in 1x PBS for 15 minutes and developed in developing solution [PBS, 0.05% (w/v) 3,3' diaminobenzidine (DAB) (Sigma), 0.06% (v/v) hydrogen peroxide] for approximately 15 minutes. Thereafter, membranes were rinsed in water, air-dried, and stored in darkness between two layers of foil.

4.8.2.2 Quantification of protein expression

Western blots for laminin-1 protein were scanned (MCID 3.0; St Catherines, ON): The relative optical density (minus background) was normalized to the loaded protein in each lane and to the sample weight. In addition, MM CK isoform levels (see section 4.8.3) were used to normalize protein expression of laminin-1 gathered from Western blots. Data

were expressed as the ratio of normalized sample optical density for deflazacort to placebo groups.

4.9 Microscopy and photography

Tissue sections prepared for *in situ* hybridization of MRF together with autoradiography (see section 4.6), for fluorescence of Evans blue dye, or for *in situ* hybridization of α2-laminin alone were observed on an Olympus BHT-2 RFCA light microscope, equipped with bright field, phase contrast and epifluorescence optics, and photographed on an Olympus C-35AD-4 camera with 400 ASA film. Black and white (TMAX 400) film was processed in T-max developer for 7 minutes, stopped for 2 minutes, fixed for 5 minutes (Kodak), washed in cold running water for 20-30 minutes, rinsed in Photo-Flo 200 solution for 30 seconds and dried. Colour slides were made using Fuji Sensia Professional film (ASA 400). For reproduction, photo negatives and slides were scanned using an Olympus ES-20 scanner and imported to Corel draw. Gel scans and scanned photographs were printed from Corel at high resolution by the Communications Systems office at the University of Manitoba.

4.10 Statistical analysis

Appropriate statistical comparisons were made using Excel (Microsoft) and NWA Statpak (Northwest Digital Inc) software according to standard criteria (Hasard, 1991). Two-way analysis of variance (ANOVA) with replication was used to investigate whether there was a significant difference in strength with deflazacort treatment over time. A probability of $p \leq 0.05$ was considered significant. Duncan's post-hoc test was used for multiple comparisons of mean strength between deflazacort- or placebo-treated mice at various times ($p \leq 0.05$). Chi-square tests ($p \leq 0.01$) were used to determine

significant differences between groups in the proportion of MRF+ proliferating mpc and CK isoform expression (normalized to muscle weight).

5. Results of Deflazacort treatment

5.1 Muscle strength

Body weight showed a slight gradual trend to increase with treatment time in both placebo and deflazacort groups. Mean body weight at the start of the experiment was 11.5 ± 0.4 g for placebo and 11.9 ± 0.3 g for deflazacort. Mean body weight at the end of the four week experiment was 22.5 ± 1.0 g for placebo and 20.2 ± 0.6 g for deflazacort.

The Chatillon apparatus (Figure 1A) was used to determine forelimb grip strength of *mdx* mice during deflazacort and placebo treatment. Measurements with the apparatus did not significantly increase the areal proportion of damaged fibers in the biceps prepared from a pilot study of mice that received intensive strength testing over a period of 1 day (Figure 1B).

The peak strength normalized to body weight (mean ± SEM) as a function of treatment time (days) for a 4 week interval was plotted (Figure 2A). *Mdx* peak grip strength, measured from 3.5 to 8 weeks-of-age, increased significantly more with deflazacort compared to placebo treatment (ANOVA and Duncan's post hoc, $p \leq 0.05$) (Figure 2A). For reference the mean peak strength of age-matched control C57BL/10 mice (C) was plotted (n=4) and was greater than peak strength in *mdx* mice.

In a repeat experiment, the mean strength normalized to body weight (mean ± SEM) was determined and plotted against time (days) for a 2 week interval of deflazacort (n=5) or placebo (n=5) treatment in *mdx* mice (Figure 2B). Both groups showed increased strength during the first 2 weeks, although mean strength was not significantly greater with deflazacort treatment. However, at 22 days (1 week after the end of treatment) the

deflazacort group had significantly greater strength than the placebo group. The strength of the deflazacort group decreased from day 22 to 29 (Duncan's post hoc, $p \leq 0.05$). At day 57 (6 weeks after the end of treatment), mice previously-treated with deflazacort again had higher strength than the placebo group of mice (Duncan's post hoc, $p \leq 0.05$). The mean strength of *mdx* mice was again lower than the strength of age-matched control C57BL/10 mice (C) at the 4 weeks treatment time.

A graph of mouse strength (relative to initial strength) was plotted over time for each mouse from the same study (Figure B*i*). Interestingly, mice that showed early increases in strength had a tendency to maintain higher strength after the end of deflazacort treatment while mice that took longer to respond to treatment tended to show the most rapid decline in strength. However, these impressions were not tested statistically. There was no difference in weight between *mdx* mice treated with deflazacort or placebo either during the 2 week treatment period or for the 6 weeks post treatment (Figure 2C).

5.2 Regeneration with deflazacort treatment

Regeneration with or without deflazacort treatment was assessed at the molecular level in muscle tissue sections and in homogenized extracts of muscle. Mpc proliferation was determined by identification of MRF mRNA-expressing mpcs using *in situ* hybridization together with autoradiography to demonstrate DNA synthesis in the same cell (see section 5.2.3). In addition, α2-laminin mRNA and laminin-1 protein expression were observed using *in situ* hybridization (see section 5.2.4.1) and immunohistochemistry (see section 5.2.4.3), respectively.

Appropriate extracts of deflazacort- and placebo-treated muscle were prepared for determination of total RNA, protein, and for immediate CK analysis. Changes in α2-

laminin mRNA and laminin-1 protein expression with deflazacort treatment were assessed using Northern (see section 5.2.4.2) and Western blots (see section 5.2.4.3), respectively.

5.2.1 Light microscopy

Extensive regeneration was present 4 days after the crush injury both in the deflazacort- and placebo-treated mice. As viewed by phase contrast (and H&E, not shown) no necrotic muscle fibers were present in the zones adjacent to the crush site in either group but some lasting necrosis was present in the central zone in the placebo-group. The adjacent zone consisted mainly of mononuclear cells and new myotubes. Surrounding the adjacent zones there were surviving myofiber segments and more mononuclear cells. Many mononuclear cells were proliferating in the adjacent zone as identified by autoradiography (Figure 3B). At day 4, the adjacent zones contained many new myotubes with central nuclei as seen by phase contrast (Figure 3C). Some myotubes could be traced to an origin at the central tendon and others were elongating from remnant myofibers. Both types appeared converged towards the central zone.

5.2.2 Creatine kinase isoforms

CK isoform levels were detected by agarose gel separation of BB (immature) from MB and MM (more mature) CK isoforms (Figure 4). Blots were scanned and the relative optical density of CK isoform activity was measured, normalized to muscle weight and the raw data expressed as percentage of total CK (%BB:MB:MM) (Table 1). All 3 isoforms were expressed in each sample. MM CK activity was compared between deflazacort and placebo groups. There was a significant shift toward MM isoform expression in both the regenerating crushed region of RTA and diaphragm with

deflazacort treatment (Chi-square, $p \leq 0.01$). With deflazacort treatment, there was an increase in expression of the MM isoform, 8% in the RTA and 9% in the diaphragm. In the diaphragm there was no change in the expression of the BB isoform with deflazacort treatment but in the RTA there was an 8% decrease. Comparably, the expression of the MB isoform was unchanged in the RTA but decreased by 9% in the diaphragm. Neither the uncrushed contralateral LTA or heart muscle showed any change in CK isoform expression with treatment.

5.2.3 Myogenic cell proliferation

The effects of deflazacort on mpc proliferation in the regenerating RTA 4 days after crush injury were investigated using *in situ* hybridization for MRFs (MyoD and myogenin) together with autoradiography to monitor new DNA synthesis. Application of this dual detection system gave rise to 3 classes of mononuclear cells. There were mononuclear cells positive for MRF mRNA (MRF+) (Figure 5A), proliferative cells with silver grains just above the plane of focus (RAG+) (Figure 5B), and proliferating mpcs identified by both RAG+ and MRF+ signals (Figure 5C). Table 2 presents the data derived from counting (where possible) at least 300 mononuclear cells in regenerating adjacent regions of RTA from each animal and group. The proliferative proportion of myogenin+ mpcs (RAG+/MRF+) in regenerating RTAs showed a significant 3.3 fold increase with deflazacort treatment (Chi-square, $p \leq 0.01$). The proportion of proliferating MyoD+ cells did not change and was very low. In addition, there was a similar increase in the proportion of proliferative mononuclear cells with deflazacort (RAG+). Negative controls (RNase pre-treated, no ^{3}H-thymidine injection) did not show *in situ* hybridization/autoradiography signal above background levels.

5.2.4 Laminin expression

5.2.4.1 *In situ* hybridization

By comparison with the assessment of proliferating mpcs, mononuclear cells were RAG+ (with silver grains just above the plane of focus) but were not positive for α2-laminin mRNA (Figure 3A and B). However, α2-laminin mRNA expression was seen in new myotubes. Both short segments and longer, more mature (larger diameter) multinucleated myotubes contained the α2-laminin *in situ* hybridization signal (Figure 3C and D). The signal for α2-laminin mRNA expression was more intense in the cytoplasm immediately surrounding and between the nuclei of myotubes. Negative controls (RNase pretreated, no ^{3}H-thymidine injection) did not show signal above background levels.

5.2.4.2 Northern blots

Alpha2-laminin mRNA expression was quantified using Northern blot analysis of homogenized extracts collected from RTA, LTA, diaphragm and heart muscles of the same groups of deflazacort- and placebo-treated mice as for the CK isoform analysis (Figure 6A). Total RNA samples were run in sequential lanes together with the 3 kb α2-chain probe serving as a positive control and size marker. Bands at the 3 kb marker were scanned and the relative optical density was compared between treatment groups (Table 3). With deflazacort treatment, α2-laminin mRNA levels (normalized to muscle weight) increased in all four muscles. Calculations with α2-laminin mRNA normalized to total RNA extracted from the samples gave similar values. The increase was largest in LTA (5.6-fold), and smallest in diaphragm (1.2-fold). When α2-laminin mRNA expression was

normalized to MM CK activity, only the RTA, LTA and heart demonstrated an increase in expression. Again LTA showed the highest increase (5.6-fold) and RTA showed a smaller increase (1.3-fold).

5.2.4.3 Protein (Western blots)

Western blot analysis of protein from pooled RTA, LTA, diaphragm and heart muscle samples of deflazacort- and placebo-treated mice were used to assess the difference in laminin-1 expression with treatment (Figure 6B). Again those were the same two groups of mice as for CK and α2-laminin mRNA (Northern Blots). Muscle extracts were run in lanes of two gels together with molecular weight markers to the right, and a laminin-1 positive control (L2020, Sigma), seen to the left (Figure 6B). After transfer, membranes were blotted with anti-laminin-1 antibody (L9393, Sigma). Preliminary results demonstrated the specificity of the polyclonal anti-laminin-1 antibody for laminin-1 in muscle tissue. Immunohistochemistry was performed according to previous reports (Anderson et al., 1991, 1993) using L9393. Laminin-1 was detected around the periphery of muscle fibers, and structures such as blood vessels in the interstitium (Figure 7).

Western blotting with the L9393 antibody demonstrated one large band between 97kDa and 116kDa and 2-3 other small bands higher and below approximately 100kDa. Bands at the 100kDa mark were scanned and the optical density compared between treatment groups. With deflazacort treatment, the expression of the laminin-1 protein increased in all four muscles, both as a proportion of muscle weight and relative to MM CK activity (Table 3). The LTA showed the largest increase in laminin-1 protein expression (5.5- and 5.6-fold respectively) while the diaphragm showed the lowest change

(1.1- fold for both). Unfortunately, laminin protein expression cold not be measured as a serial dilution of laminin standard on the blots was not successful and ratios of deflazacort: placebo were therefore presented (Table 3). Deflazacort vs. placebo ratios were similar in magnitude for Western and Northern analyses of protein and mRNA respectively.

Figures and Tables

Figure 1

A. Apparatus used to administer strength tests. Forelimb grip strength (peak or mean peak strength) was measured in grams with a Chatillon gauge and normalized to body weight.

B. A representative cross-section of muscle from the right forearm of an *mdx* mouse (8 weeks of age) stained with Evans Blue 20 hours prior to sacrifice and after one day of strength testing. The dye is excluded from intact muscle fibers but penetrates disrupted fiber membranes (bottom right corner) allowing for the assessment of damage by fluorescence microscopy. No differences were apparent in the relative area of florescent fibers between animals with or without strength testing.

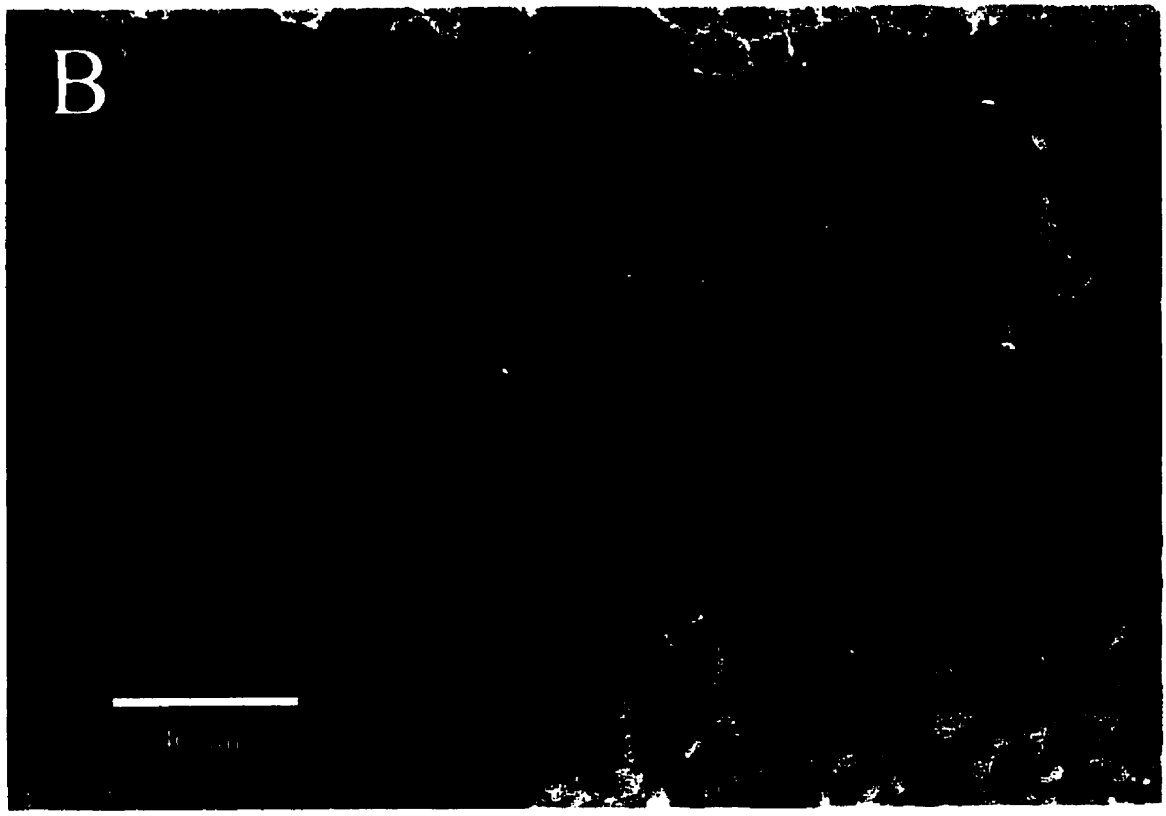
B

Figure 2

A. Graph of normalized (Norm.) peak strength (mean ± SEM) as a function of treatment time (days) in mice treated with deflazacort (n=13) and placebo (n=14). The treatment interval is indicated (Rx) on the x-axis. Grip strength was measured from 3.5 to 8 weeks-of-age, before and during 4 weeks of treatment with deflazacort or placebo. Normalized peak strength increased significantly more with deflazacort than with placebo treatment (ANOVA and Duncan's post hoc, $p \leq 0.05$). Mean peak strength of age-matched 8-week-old control C57BL/10 mice (c) is indicated at day 28.

*Indicates significant difference between deflazacort- and placebo-treated mice (Duncan's post hoc, $p \leq 0.05$)

B. Graph of normalized (Norm.) mean strength (mean ± SEM) as a function of treatment time (Rx arrow) in deflazacort (n=5) and placebo (n=5) groups of *mdx* mice. Mean grip strength was measured from 3.5 to 11.5 weeks-of-age, during and 6 weeks after treatment. Overall, mean strength increased significantly more with deflazacort compared to placebo treatment (ANOVA, $p \leq 0.05$). Pair-wise differences between groups were noted at day 22 (one week post-treatment) and again at day 57 (6 weeks post-treatment) ($p \leq 0.05$). Initial changes in strength from day 0 to 5 and then 5 to 10 were present for both deflazacort- and placebo-treated mice ($p \leq 0.05$). However, only those mice treated with deflazacort showed an increase in strength after the end of treatment from day 15 to 22 and a subsequent decrease in strength from day 22 to 29 ($p \leq 0.05$). Mean strength of 8-week-old control C57BL/10 mice (C) is indicated at day 29.

B*i*: Graph of mean strength (normalized as a ratio of the first strength reading at day 0) plotted as a function of treatment time (days) in the same group of deflazacort-treated *mdx* mice (n=5) as shown in Figure 2B. Deflazacort-treated *mdx* mice that showed the most rapid increase in strength at the start of treatment seemed to maintain strength longer once treatment was stopped.

*significant difference between deflazacort- and placebo-treated mice (Duncan's post hoc, $p \leq 0.05$)

✦significant difference between two consecutive strength measurements of deflazacort-treated mice ($p \leq 0.05$)

✧significant difference between two consecutive strength measurements of placebo-treated mice ($p \leq 0.05$)

C. Graph of body weight (g) (mean ± SEM) as a function of treatment time (days) in the same two *mdx* mice groups of panel B. Weight was recorded from 3.5 to 11.5 weeks-of-age. Weight did not differ between treatment groups (ANOVA).

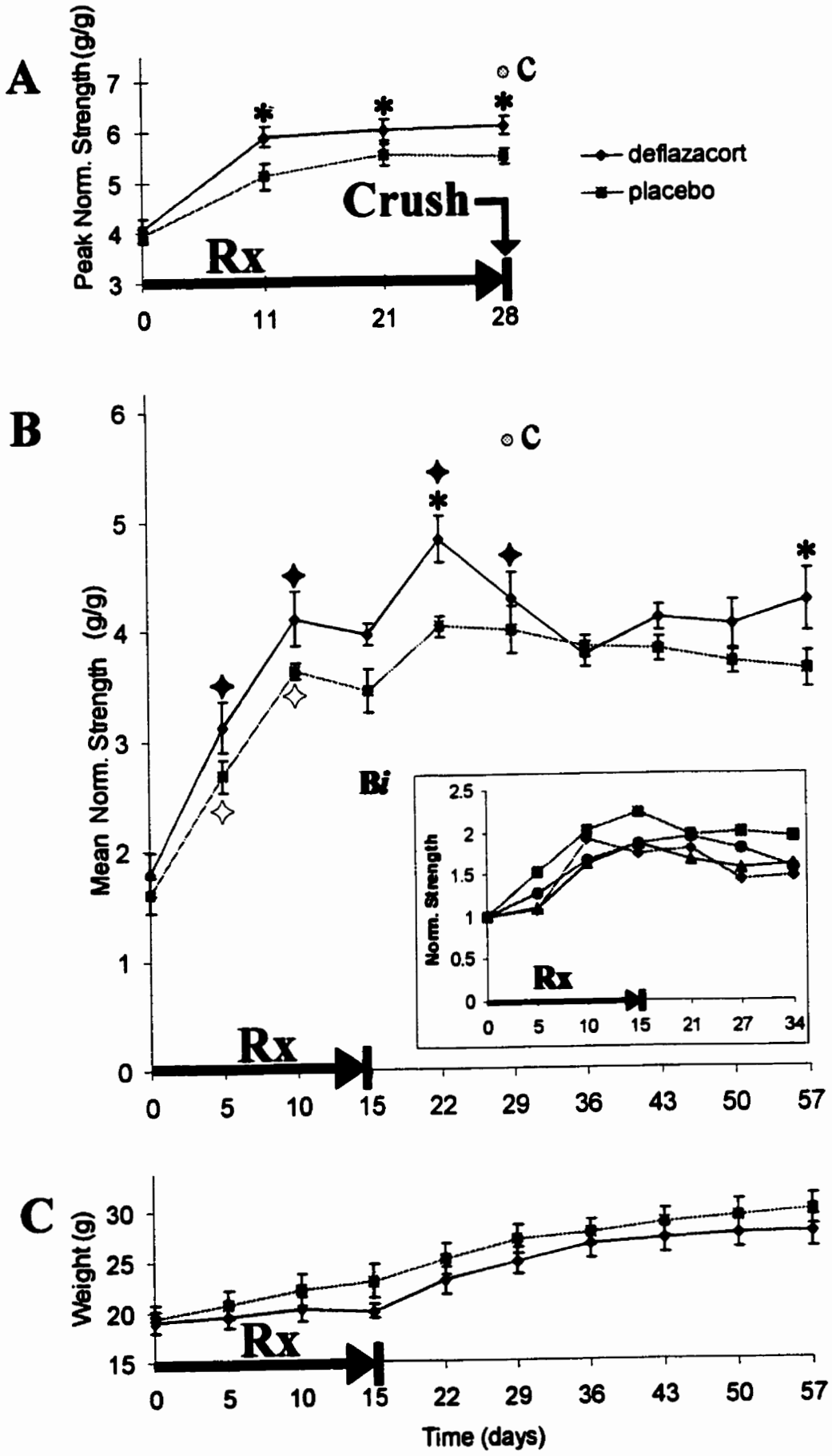
A
Peak Norm. Strength (g/g)
C
deflazacort
placebo
Crush
Rx
B
Mean Norm. Strength (g/g)
Bi
Norm. Strength
C
Rx
Rx
C
Weight (g)
Rx
Time (days)

Figure 3

Regenerating RTA muscle was examined four days after crush injury by *in situ* hybridization for α2-laminin mRNA expression, and for proliferation by detection of incorporated tritiated thymidine. Representative sections are shown in two views with phase contrast (A and C) or bright field (B and D) optics.

A and B (same field): Many mononuclear cells are present within the regenerating muscle (A) and some are making DNA and labeled with silver grains (A and B, arrowheads). No mononuclear cells expressed α2-laminin mRNA (A and B, arrows).

C and D (same field): Alpha2-laminin mRNA is detected in long multinucleated myotubes and in shorter myotubes with only two nuclei visible (arrows). The α2-laminin signal is most intense in the cytoplasm directly surrounding the nuclei of the newly-formed myotubes.

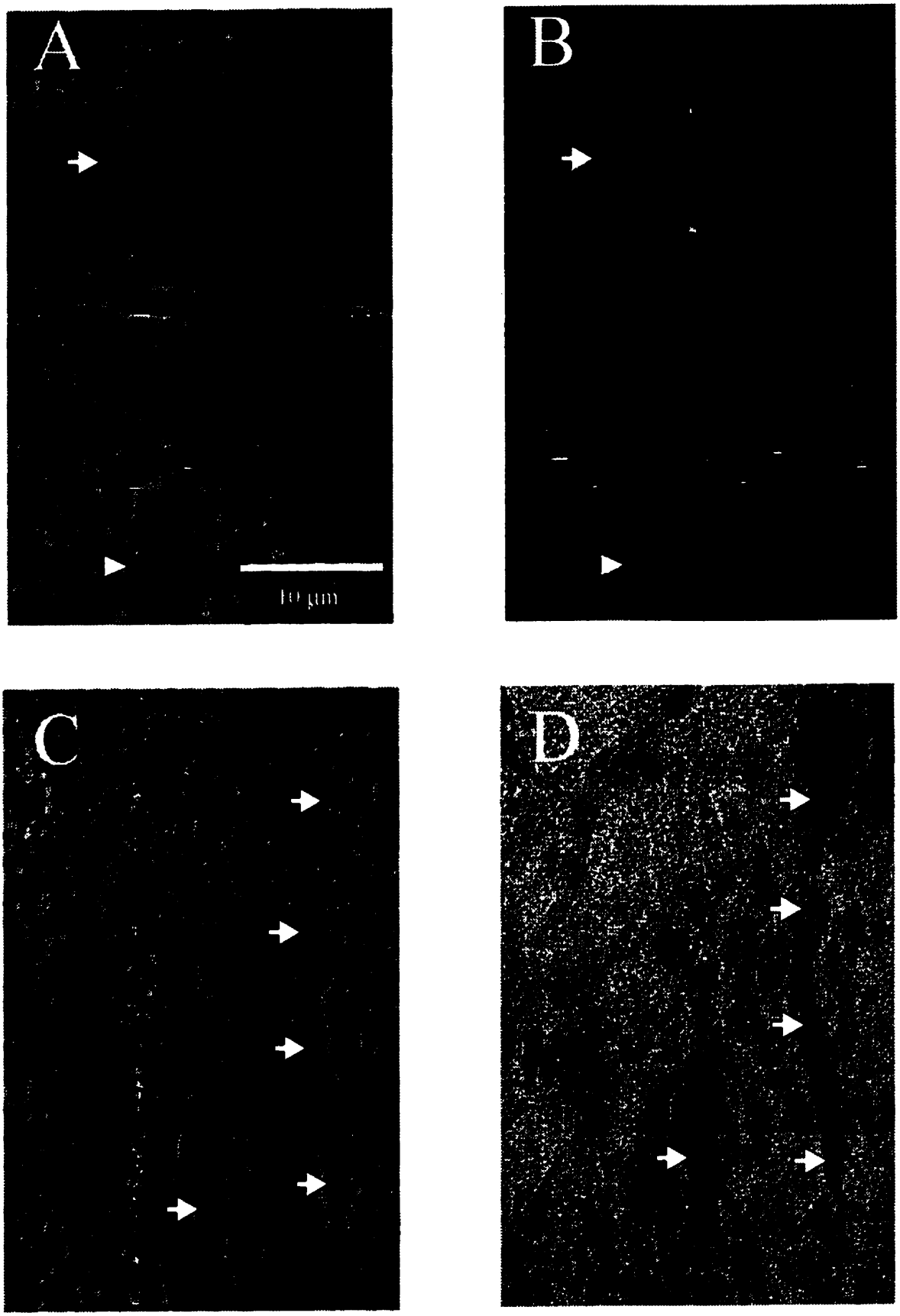
A
B
C
D
10 µm

Figure 4

Creatine kinase isoform levels (BB, MB, MM) as detected by zymogram on agarose gels for pooled RTA, LTA, heart and diaphragm muscles of deflazacort-treated (Rx) (+) and placebo-treated (-) groups.

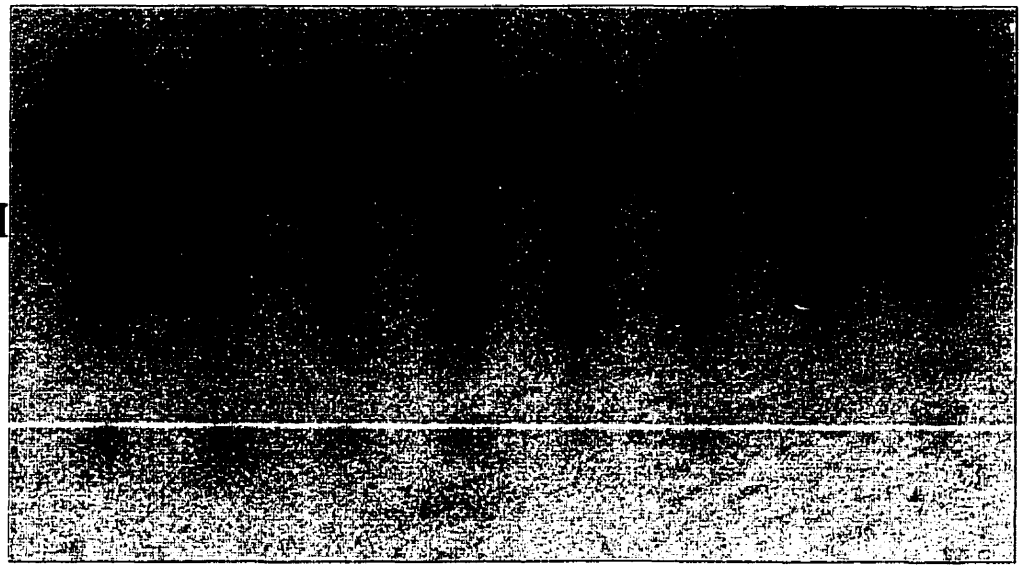

Muscle	RTA		DIA		Ht		LTA	
Rx.	+	-	+	-	+	-	+	-

Table 1

Optical density (minus background density) of CK isoforms BB:MB:MM (column 1), and CK isoform optical density normalized to muscle weight and expressed as a percentage of total CK, %BB:MB:MM (column 2). After deflazacort treatment, the regenerating RTA and diaphragm muscle showed a significant shift toward mature MM CK isoform expression (Chi-square, $p \leq 0.01$).

	1. Density (BB:MB:MM)		*2. Density/wt. (%BB:%MB:%MM)*	
Muscle	**Placebo**	**Deflazacort**	**Placebo**	**Deflazacort**
RTA	185:278:395	164:351:617*	22:32:46	14:31:55
LTA	179:332:572	158:264:461	17:31:53	18:30:52
DIA	154:408:402	139:267:402*	16:42:42	17:33:50
Ht	158:366:335	172:415:364	18:43:39	18:44:38

* Indicates significant difference (Chi-square, $p \leq 0.01$)

Figure 5

A representative field of mononuclear cells in the regenerating RTA of a deflazacort-treated *mdx* mouse. Mpcs are positive for A) MyoD mRNA (MRF+), B) silver grains just above the plane of focus (RAG+) in proliferative cells and, C) proliferating mpcs, identifiable by both RAG+ and MRF+ signals.

Table 2

Data from combined *in situ* hybridization and autoradiography experiments to detect MRF expression (MRF+), either MyoD or myogenin, in proliferating (RAG+) cells. The proportions of RAG+, MRF+ (MyoD or myogenin) and proliferating mpcs (RAG+/MRF+) in regenerating RTAs of *mdx* mice treated with deflazacort (n=22) or placebo (n=17) are shown. With deflazacort, the proliferative proportion of myogenin+ but not MyoD+ mpc increased (Chi-square, $p \leq 0.01$).

Mean ± SEM	**RAG+ (≥5 grains)**	**MRF+**	**RAG+ /MRF+**
MyoD			
Placebo (4849)[a]	0.033 ± .013	0.953 ± .018	0.014 ± .006
Deflazacort (7258)	0.079 ± .022	0.895 ± .029	0.026 ± .008
Myogenin			
Placebo (614)	0.092 ± .003	0.888 ± .003	0.020 ± .0001
Deflazacort (7511)	0.305 ± .053	0.629 ± .057	0.067 ± .011*

a: the number in brackets indicates total number of cells counted for each treatment group

* Indicates significant difference (chi-square, $p \leq 0.01$)

Figure 6

A. Northern blots of total RNA from *mdx* muscles after 4 weeks of treatment with deflazacort (+) (n=13) or placebo (-) (n=14). RTA, LTA, diaphragm and heart muscles were probed for α2-laminin mRNA and signal was detected with chemiluminescence on X-ray film. Size marker for 3kb is shown on the right.

B. Western blots of protein extracted from the same set of muscles (above and Figure 4) treated with deflazacort (+) (n=13) or placebo (-) (n=14). RTA, LTA, diaphragm and heart muscles were immunoblotted with L9393 antibody for laminin-1 (Sigma). Molecular weight markers for 116kDa and 97kDa are indicated on the right. A laminin-1 (Lam) standard is indicated in the first lane on the left as the positive control.

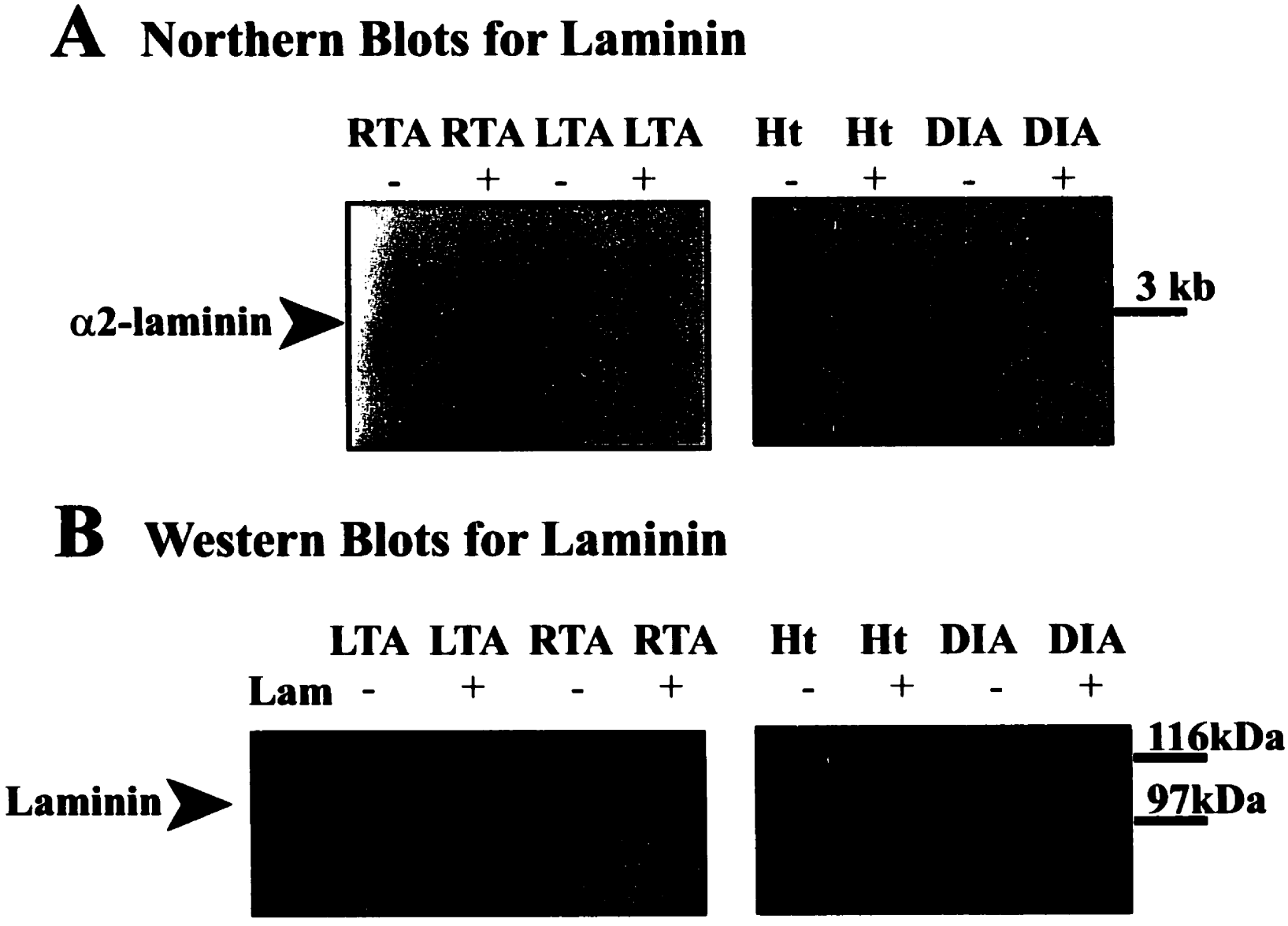
A Northern Blots for Laminin
RTA RTA LTA LTA
- + - +
Ht Ht DIA DIA
- + - +
α2-laminin
3 kb
B Western Blots for Laminin
LTA LTA RTA RTA
Lam - + - +
Ht Ht DIA DIA
- + - +
Laminin
116kDa
97kDa

Table 3

Data for the ratios of α2-laminin mRNA (Northern) and laminin-1 protein (Western) expression for deflazacort to placebo samples. Data were normalized to muscle weight (mg), or to muscle weight and the proportionate MM CK activity from the same muscles. With deflazacort treatment, α2-laminin mRNA levels increased in all four muscles. Alpha2-laminin expression relative to MM CK activity was increased only in RTA, LTA and heart. With deflazacort treatment, laminin-1 protein expression increased in all four muscles both as a proportion of muscle weight and relative to MM CK activity.

Deflazacort/ Placebo	**Northern**		**Western**	
Muscle	**OD/RNA/ Wt**	**OD/RNA/ wt/MM**	**OD/Protein/ wt**	**OD/Protein/ wt/ MM**
RTA	1.52	1.29	1.63	1.38
LTA	5.57	5.63	5.49	5.56
DIA	1.17	0.98	1.06	1.08
Ht	2.07	2.08	2.11	1.77

Figure 7

A cross section of LTA muscle from an untreated *mdx* mouse. Immunostaining using the anti-laminin-1 antibody L9393 (Sigma) localized the signal to the periphery of myofibers. The inset is a negative control prepared without the primary antibody.

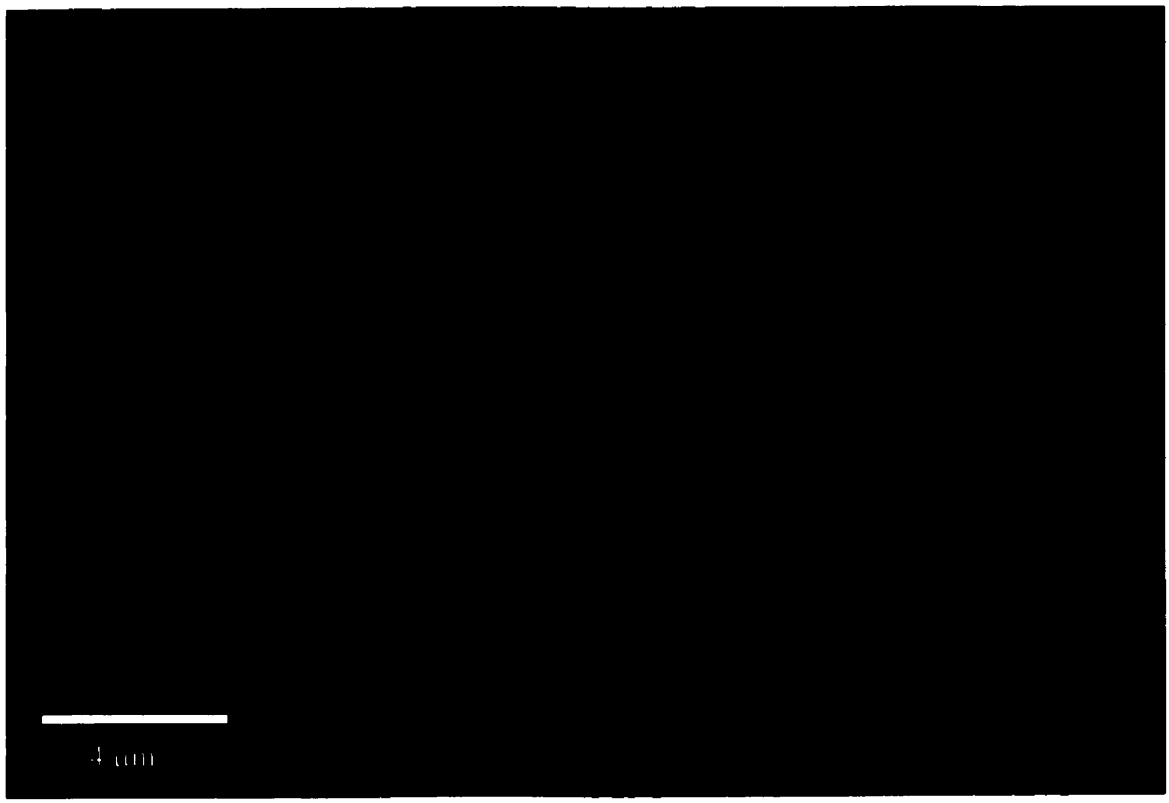

6. Discussion

We accept our overall hypothesis. Results showed that deflazacort promoted gains in strength during and after treatment. Deflazacort also increased the proliferation of myogenin+ mpcs and myogenic differentiation in regenerating dystrophic muscle (shift to MB/MM CK expression). Finally, deflazacort increased α2-laminin mRNA and laminin-1 protein expression. These results suggest there could be multiple target sites for deflazacort in the muscle cell. Further research is needed to determine the time course and duration of the deflazacort effect on regeneration and function.

6.1 Functional effects of deflazacort

We have demonstrated that after 4 weeks of treatment with deflazacort (compared to placebo), *mdx* grip strength was increased. As well, in an additional 2-week study, we observed the beneficial effect of deflazacort to occur 1 week post-treatment. During the next 5 weeks in this same study, regression in the strength of the deflazacort-treated mice was observed. However, following this decline, grip strength increased once again. Hudecki et al. (1993) in a previous 8 week study with prednisone (from 5 to 13 weeks-of-age) demonstrated that *mdx* strength increased after treatment. In that study whole body strength was measured many times during treatment by tying the tail of the mouse via a non-flexible nylon thread to a force transducer. Unlike the past study, the present experimental design took into consideration normal growth patterns and natural disease progression by recording strength of *mdx* mice early in life (3.5 to 8 weeks-of-age) from the time of disease onset and when disease severity and the similarity to DMD were the greatest. In addition, using Evans blue infiltration to indicate fiber damage, we were able

to confirm that the present method of testing strength did not appear affect the integrity of the forelimb muscles. Therefore our results can be considered a true representation of treatment and not due to damage caused by strength testing itself. This was not examined or ruled out by Hudecki et al. (1993), who looked at changes in fiber diameter in mice tested for endurance on a treadmill, and did not examine the integrity of the muscles during strength testing. In addition, the reliability of the protocol used by Hudecki et al. (1993) is questionable; it had a small sample size (N=3), and did not indicate the sex of the animal. Hudecki et al. (1993) normalized force to body weight similar to the present study. However, only the present study demonstrated there was no difference in weight between *mdx* mice treated with deflazacort or placebo either during the 4-week treatment study or during the 2-week treatment period and the 6 weeks after treatment. There was a consistent trend for deflazacort-treated mice to weigh less than the placebo groups. However, we noted no fluctuations in weight in the inverse direction from those of the mean strength changes that would explain the strength changes recorded as normalized to body weight. Therefore, the changes in strength could be attributed to the treatment effect and not to any difference in weight between groups, which would have affected the ratio of strength normalized to body weight.

Anderson et al. (1996), Hudecki et al. (1993) and the present study together demonstrated that in *mdx* mice treated with glucocorticoids muscle strength, central nucleation and fiber diameter increased while the inflammation of dystrophy decreased. In contrast, Weller et al. (1991) saw no change in the prevalence of necrosis or regeneration in *mdx* muscle and did not examine whether mice treated with glucocorticoids showed increased strength or altered muscle function. Structural changes

in muscles of *mdx* mice treated with glucocorticoids are studied because of the obvious difficulties in studying muscle of treated DMD boys who show functional benefits of treatment. Therefore, because Weller et al. (1991) did not perform functional tests on *mdx* mice treated with a variety of glucocorticoids, the absence of structural changes in their study can not be corroborated by their evidence. In addition in that study, there was no explanation why different concentrations of drug were administered, why the dose was changed (i.e. cyclosphamide was administered at 10mg/kg of body weight for the first 2 days and then at 3mg/kg of body weight twice a week) and the rationale for the treatment schedule. They also looked only at soleus and plantaris (not representative fast muscles, diaphragm and heart) and at central nucleation, fiber number and serum CK levels. Anderson et al. (1996), Hudecki et al. (1993) and the present findings clearly show that muscle strength in *mdx* mice increased with glucocorticoid treatment as it does in patients with DMD, and that the morphological changes provide substantial bases for that gain in strength. This also shows that the *mdx* mouse is a good model for the study of DMD treatment counter to discussion by Weller at al. (1991), provided that adequate testing occurs to give evidence of treatment effects.

Brooke et al. (1987) reported a functional grade test for DMD patients and showed that glucocorticoid treatment slowed the deterioration of muscle strength and functional mobility. Our experimental procedure was similar to the experiment by Brooke and colleagues, and demonstrated that there could be continuing increases in strength without re-administering deflazacort. This has significant clinical application as there are many inherent negative side effects associated with prolonged glucocorticoid treatment (Khan, 1993; O'Connell et al., 1993). In brief, we have seen that the beneficial effects of

treatment can be maintained after treatment is discontinued, although there was a gap between the 2 time periods when strength was found to be increased relative to the placebo group. Presumably the second rise in strength may occur without the associated side effects or at least side effects of lesser and decreasing severity than during treatment. As well, since deflazacort has effects on intact muscle as well as on muscle growth during repair (Anderson et al., 1996), the strength changes for those 2 types of muscle may not occur at the same time. The second increase in strength, some 6 weeks after the end of treatment may relate to increases in fiber growth. As well, an increased number of satellite cells (Anderson unpublished data) could have responded to dystrophy since the end of treatment to increase fiber number, and the increases in laminin expression may also continue or persist after treatment to stabilize fibers and thereby potentially contribute to increased strength. Following from these data, patients suffering from DMD could be placed on deflazacort for a set period of time to allow their overall strength to increase, and then be given a 'medication holiday' to minimize adverse reactions and allow the body to regain its normal homeostatic endocrine balance. This would allow for a cyclic treatment schedule with deflazacort, which could be administered for a period of time and then discontinued. Such a treatment plan could exploit the beneficial effects and hopefully minimize the side effects of deflazacort treatment.

Another potential means of increasing strength while avoiding the negative effects of deflazacort would be to further probe for the molecular mechanisms such as the involvement of glucocorticoid receptors, responsible for the observed increases in strength and myogenic repair, and exploit the knowledge in a new treatment strategy. Other drugs could be designed to have the same functional benefit perhaps without the

associated side effects of deflazacort. Deflazacort, an oxazoline derivative of prednisone has fewer side effects than its parent compound (O'Connell et al., 1993). However, the feasibility of designing a steroid with no side effects would be challenging due to the inherent actions of steroids, since it is not known why deflazacort has less adverse effects than prednisone.

6.2 Structural effects of deflazacort

A close investigation of particular aspects of dystrophy and repair during deflazacort treatment was performed to determine the possible gene and cellular targets of this drug.

6.2.1 Creatine kinase isozyme expression

Predictable, progressive changes in the CK isoform pattern of expression throughout regeneration and the abundance of this enzyme make CK isoform analysis an ideal index for monitoring muscle regeneration (Bischoff and Heintz, 1994). Because the shift from BB (immature) to MM (more mature) isozymes occurs during a 2-4 day interval period after injury (Bischoff and Heintz, 1994), experiments were designed to sample regenerating muscle at exactly this time when the earliest myotubes were differentiating. CK isozymes, MRF+ mpc proliferation, and laminin expression were all examined in the same group of muscles after either placebo or deflazacort treatment for 4 weeks. The possible changes in these parameters after only 2 or 3 weeks of deflazacort treatment may also now be of interest due to results of the short-term study of deflazacort treatment on muscle strength.

The standard serum assay of CK activity detects the CK that has leaked from damaged muscle cells, for example as a clinical marker of DMD or myocardial

infarction. In this study, the CK isoform activity of muscle itself was investigated to study muscle differentiation directly. With deflazacort treatment, the regenerating RTA demonstrated a relative shift from predominantly BB or MB to MM isoforms, therefore representing a greater amount of more mature skeletal muscle myotubes in the regenerating samples. The diaphragm of deflazacort-treated *mdx* mice also demonstrated an increase in MM CK isoform activity relative to total CK activity. The diaphragm of the *mdx* mouse is more severely affected by dystrophy than the limb muscles (Stedman et al., 1991), and exhibits lasting abnormalities as well as fibrosis (Anderson et al., 1998). However, with deflazacort treatment the diaphragm is less inflamed, shows a greater number of newly-formed fibers and larger mean fiber diameter, and importantly, shows a less severe phenotype of *mdx* dystrophy (Anderson et al., 1996). It is therefore reasonable that we observed an increased expression (assayed by activity) of mature MM CK isoforms in the diaphragm with deflazacort treatment. Indirectly this means that the diaphragm samples contained more mature skeletal muscle because of the beneficial effects of deflazacort as demonstrated by the drug effects on regeneration in the diaphragm.

6.2.2 Muscle precursor cell proliferation

The effects of deflazacort on mpc proliferation were examined using *in situ* hybridization for MRF mRNA expression (MyoD or myogenin) and autoradiography, in combination on the same tissue sections. With deflazacort treatment we measured a 3.3-fold increase in the proportion of proliferating myogenin+ mpcs, but no change in the proliferation of MyoD+ mpcs. MRFs are muscle-specific transcriptional regulators that are expressed before DNA synthesis occurs in regenerating muscle. Expression of MRFs can convert non-determined cells like fibroblasts to myoblasts in the muscle lineage and

eventually from myotubes from myoblast fusion (Weintraub et al., 1989). MyoD acts early in myogenesis and is required for cell determination or commitment, while myogenin acts later and is responsible for cell differentiation (reviewed in Megeney et al., 1996; Rudnicki et al. 1993). Grounds et al. (1992) demonstrated how mpc could be identified using *in situ* hybridization for MyoD and myogenin *in vivo*. Using an innovative approach (both *in situ* hybridization and autoradiography) reported from this laboratory (McIntosh et al., 1998; Anderson et al., 1998) we have been able to monitor the effects of deflazacort on the proliferative proportions of mpcs.

Deflazacort increased the proliferative proportion of mpcs expressing myogenin. This can be taken as an indicator that deflazacort promoted proliferation of differentiated mpcs in the regenerating RTA muscle. Interestingly, deflazacort did not increase the proliferation of mpcs expressing MyoD. Satellite cells are reported to respond to injury within 4-8 hours after an insult, as observed by the expression of myogenin and MyoD (Rantanen et al., 1995). It is therefore curious that expression in proliferating mpcs of one MRF (myogenin) but not the other (MyoD) would be greater after deflazacort treatment although the shift to increased differentiation is consistent with the change. An increase in mpc proliferation with deflazacort treatment means an increase in the number of precursor cells, which are available to fuse and form myotubes. This in turn would augment the regenerative process and ultimately increasing the number of myofibers. The present study was concerned with the cycling of mpcs during expression of MyoD and myogenin, rather than whether or not potential precursors are committed to muscle (i.e. determined). Therefore one could speculate that if the proliferation of only myogenin+ mpcs is increased, it suggests that myogenin but not MyoD may be responsive (directly

or indirectly) to glucocorticoids. It is possible that only the myogenin gene has a glucocorticoid response element in the promoter sequence or maybe only myogenin+ mpcs can respond to increase laminin expression by myotubes that differentiate immediately following myogenin expression and a final wave of mpc proliferation. Since laminin and integrins are now known to take part in signal transduction pathways (see below), responses to laminin by differentiated (myogenin+) mpcs, possibly by increased adhesion or mobility or increased fusion, could induce better repair. It is also possible that because of the high background on many slides probed for MyoD mRNA, a real increase in MyoD+ mpc proliferation was not detected. Alternatively, MyoD expression could be very short or, MyoD mRNA may have a shorter half-life compared to myogenin, making it very difficult to detect an increase (if it did happen) using the autoradiography and *in situ* hybridization method. Our laboratory has previously demonstrated that *mdx* muscle has higher levels of proliferation by myogenin+ than myf5+ cells (Anderson et al., 1998, McIntosh et al., 1998), which is consistent with the present data. However, further studies are needed in order to determine the exact reasons that explain why the proliferative proportion of myogenin+ mpcs but not MyoD+ mpcs was increased.

6.2.3 Laminin expression

Alpha2-laminin (α2-chain-containing laminin) is the major isoform of laminin found in adult skeletal muscle basement membranes (Ehrig et al., 1990). Absence of the α2-chain induces a type of muscular dystrophy in dy/dy mice (Xu et al., 1994), and defects in the α2-chain in humans cause congenital muscular dystrophies (Allamand et al., 1997; Helbling-Leclerc et al., 1995). A lack of dystrophin in *mdx* mice and DMD

muscle results in the loss of associated proteins including α2-laminin (Ervasti et al., 1990; Ohlendieck et al., 1991) since the dystroglycan complex is constituted in relation to the presence or absence of dystrophin. In addition, in DMD or *mdx* myotubes, α2-laminin-mediated adhesion is defective (Angoli et al., 1997). These background studies highlight the importance of α2-laminin contributing to the structural integrity of muscle at least in the presence of dystrophin, although it could be argued that increased laminin expression alone may also stabilize fiber membranes (see below).

Prior to the current knowledge on the different isoforms of laminin, immunohistochemistry studies were performed on human and rabbit epithelium and smooth muscle tissue using the 4C7 antibody, a monoclonal antibody raised to placental laminins. The 4C7 antibody is considered not to react with laminins that contain the α2-chain, but with a α1-chain-containing laminin-1 (α1, β1, γ1) in humans as well as in non-human species (horse and rabbit, but not mouse) (Engvall et al., 1986; Engvall et al., 1990). Alpha1-chain-containing laminins are not typically recognized as a laminin isoform of muscle. Usually α2-laminin (containing the α2-chain) is thought to be present in muscle. However, α1-chain-containing laminins bind with the 4C7 antibody, and have been detected in the basement membrane of normal muscle as well as in the blood vessels of muscle tissue (Sewry et al., 1995). In addition, α1-chain-containing laminins have been reported to stimulate proliferation, motility, and the development of muscle cells *in vitro* (von der Mark and Ocalan, 1989; Goodman et al., 1989; Echtermeyer et al., 1996). Importantly, the expression of the α1-chain of laminin also increases in some muscular dystrophies (Sewry et al., 1995; Mundegar et al., 1995; Sunada et al., 1995). It seems plausible that in certain forms of muscular dystrophy, different isoforms of laminin may

compensate for the defect or decrease in α2-laminin, and decrease the severity of the disease. It is also possible that deflazacort itself may increase the expression of certain isoforms of laminin in dystrophic *mdx* mice, especially since there is a glucocorticoid response element in the promoter region of α2-laminin (Simo et al., 1992). However it is not known whether membranes would be more stabilized by α2- or α1-laminins.

Simo et al. (1992) demonstrated how treatment with a glucocorticoid could increase the expression of laminin in mesenchyme-derived cells, and we have hypothesized that deflazacort treatment would increase laminin expression in dystrophin deficient *mdx* mice, thereby aiding in the regenerative process. The dystrophin-glycoprotein complex is in direct association with laminin in the extracellular matrix outside the cell, and with dystrophin beneath the sarcolemma within the cell. Although dystrophin is still absent in *mdx* mice, an increase in laminin expression with deflazacort treatment may still improve fiber stability and repair, not by utilizing dystrophin but possibly by utilizing utrophin. Utrophin has high sequence homology with dystrophin and has been suggested to functionally compensate for the lack of dystrophin (Love et al., 1989). It is thus possible that utrophin can partly compensate for the lack of dystrophin, and together with the increase in laminin result in a less severe phenotype of dystrophy.

Besides α-dystroglycan, a 156-kDa protein member of the dystrophin-glycoprotein complex (Gee et al., 1993), a high affinity laminin receptor of 67 kDa has been found and isolated from several tumor cells, myoblasts, and other primary cells (Liotta et al., 1986; von der Mark and Risse, 1987; Sobel, 1993). In addition to these non-integrin receptors there are integrin receptors which are involved in the specific adhesion of cells to laminin. There are five laminin-binding integrins of the β1 family, which

recognize different sites and isoforms of laminin. The major laminin-binding integrin isolated from murine skeletal myoblast is α7β1 (von der Mark et al., 1991; Song et al., 1992) which exists in three cytoplasmic and two extracellular splice variants (Song et al., 1993; Ziober et al., 1993). Therefore, although dystrophin is still absent in *mdx* mice, through many different receptors on the cell surface as well as a possible compensatory role utrophin may play in the dystrophin-deficient mice, an increase in laminin expression with deflazacort treatment may help to stabilize muscle fiber membranes and improve repair in dystrophic muscle.

6.2.3.1 Alpha2-laminin mRNA expression

Sections from regenerating RTA muscles were prepared for *in situ* hybridization for the mRNA sequence of the α2-chain of laminin. Alpha2-laminin mRNA was identified in multinucleated myotubes but not in mononuclear cells. The localization of α2-laminin to the cytoplasm of more mature differentiated myotubes rather than mononuclear cells (including mpcs) indicated that α2-laminin mRNA was transcribed during or after fusion of mononuclear cells. It therefore seems reasonable that α2-laminin, an essential component of the basement membrane, is expressed during remodeling once the myotubes have formed. No attempt was made to quantify the expression of α2-laminin mRNA in tissue sections because α2-laminin mRNA was localized not to mononuclear cells but myotubes and myofibers of varying size making quantification for example, of staining intensity difficult. In addition, the *in situ* hybridization studies were made on a different set of tissue samples than mRNA, protein, and CK experiments due to laboratory mishaps.

Total RNA from homogenized RTA, LTA, diaphragm and heart muscle samples was prepared for Northern blot analysis and probed for α2-laminin sequence to provide information on the average content of α2-laminin in the muscle homogenates. The RTA tissue samples were derived only from the regenerating region of crushed RTA containing new myotubes, and did not include the surviving fiber segments outside the damaged region, where laminin would be stably expressed. With deflazacort treatment, there was an increase in α2-laminin mRNA normalized to muscle weight in all four muscles relative to the placebo group. When α2-laminin mRNA levels were further normalized relative to proportionate MM CK activity, to find changes in α2-laminin expression relative to new muscle content in the same muscles, only the RTA, LTA and heart demonstrated an increase in expression. However values were semi-quantitative, as no internal standard was used to ensure loading conditions did not change.

During regeneration, the basement membrane acts as a scaffold for the synthesis of new myofibers (Bischoff, 1990; Hughes and Blau, 1990). However, α2-laminin (an essential component of the basement membrane) is down-regulated in both DMD and *mdx* mice where continuous degeneration and regeneration of muscle is actively occurring and in the absence of dystrophin (Ervasti et al., 1990; Ohlendieck et al., 1991). This is possibly secondary to loss of dystrophin, in addition to progressive loss of mature muscle from the samples. Our investigation distinctly demonstrated that deflazacort treatment was accompanied by an increase in expression of α2-laminin mRNA in pooled homogenized muscle extracts. Alpha2-laminin expression may be one of the direct molecular targets of deflazacort action and could secondarily contribute to the observed increase in strength in the treated mice.

6.2.3.2 Laminin-1 protein expression

The 4C7 antibody used to identify laminin-1 (α1, β1, γ1) in human congenital muscular dystrophies does not react with the α1-chain in mice. Therefore in order to assess the effects of deflazacort on α1-chain-containing laminins in *mdx* dystrophic mice, we used the Sigma antibody L9393. This antibody was developed against laminin from purified Engelbreth-Holm-Swarm tumor (L2020; 100kDa by SDS-PAGE, Sigma) which is now designated as laminin-1 (Tiger and Gullberg, 1997). Immunohistochemistry was used to positively demonstrate the specific localization of laminin-1 as detected using L9393, to the periphery of skeletal muscle in *mdx* mice.

In this study Western blot analysis of homogenized RTA, LTA, diaphragm, and heart muscles using the L9393 antibody revealed a distinctive high-density band between molecular weight markers 97kDa and 116kDa, corresponding roughly to 100kDa. This band may represent the 100kDa G-domain (globular domain) at the C-terminus of the α1-chain of laminin-1. However, since L9393 is a polycolonal antibody there was more than 1 band in the Westerns (approximately at 400kDa, 200kDa 90kDa and 50kDa) and therefore more than 1 domain of laminin-1 was recognized by the antibody. We chose to measure the relative expression of the 100kDa band, as it was the largest and most consistent band, both in the muscle samples and the positive control (laminin-1, L2020). Laminin-1 expression in the pooled RTA muscle samples from deflazacort-treated mice in this study was increased compared to placebo both as a proportion of muscle weight and relative to MM CK activity. Northern blots showed increased expression of α2-laminin mRNA, and Western blots showed increased expression laminin-1 protein with deflazacort treatment in the RTA (both relative to placebo). There was also a greater

relative expression of each molecule in LTA compared to RTA and the relative increase was greater in LTA than RTA with deflazacort treatment compared to placebo treatment.

The greater relative increase in laminin expression in the uncrushed LTA compared to the regenerating RTA may be due to the time course of laminin expression. Laminin is found at the periphery of myofibers, yet at day 4 after the crush injury to the RTA, there is much less muscle present. The muscle that is present is made up of small myotubes while the mononuclear cells that are also present at 4 days do not express α2-laminin mRNA, as seen by *in situ* hybridization. By comparison, there are many large mature myofibers in the LTA of *mdx* mice and they do express the laminin-1 protein as observed by immunohistochemistry. Therefore, the change in deflazacort:placebo ratio was observed to be the greatest in the LTA where there was the greatest amount of mature muscle present. We would expect the levels of α2-laminin mRNA and laminin-1 protein to increase further in the RTA after sufficient time has elapsed for myotubes to mature and grow and for further remodeling of the encompassing extracellular matrix to occur.

Deflazacort was observed to have the least effect on the expression of both α2-laminin mRNA and laminin-1 protein in the diaphragm, with a slight decrease in normalized relative mRNA expression compared to placebo. The diaphragm exhibits more severe dystrophy than limb muscles, and like the crushed RTA is undergoing regeneration. However, unlike the RTA, the diaphragm has been observed to have much less new myotube formation in dystrophy-induced repair than RTA in injury-induced regeneration (Anderson et al., 1998), and diaphragm is also said to have a lower regenerative capacity than TA. Therefore the lower expression of laminin in diaphragm

than LTA may reflect the lower extent of muscle regeneration and lower proportion of muscle tissue in total muscle weight in diaphragm than LTA. Unlike the situation in LTA where there is a large proportion of stable unaffected myofibers at 8 weeks-of-age, the diaphragm muscle contains an asynchronous collection of regenerating myofibers and scar tissue. It is possible that matrix protein changes are not detectable relative to muscle weight or MM CK and should be measured relative to collagen expression in scar tissue. Alternatively, the very small but mature diaphragm fibers may be less able to modify matrix synthesis than limb muscle fibers, possibly due to demands for continuous rhythmic contractions and fiber flexibility and consequent metabolic demands of that activity.

Interestingly, expression of both α2-laminin mRNA and laminin-1 protein were increased in dystrophin-deficient *mdx* muscle by the actions of deflazacort. Perhaps the presence of laminin-1 in dystrophic muscle is an important means of compensating for the lack of dystrophin, aiding α2-laminin stabilization of the sarcolemma. Only α2-laminin, and not laminin-1 was observed to decrease apoptosis and promote survival in normal muscle (Vachon et al., 1996), and therefore an increase in both α2-laminin and laminin-1 together with a beneficial increase in strength with deflazacort treatment may be surprising. Vachon et al. (1996) reported on normal myotubes, however, the present study was on dystrophic *mdx* muscle. Therefore the lack of dystrophin in *mdx* mice may be so detrimental to membrane function or integrity that an increase in both α2-laminin and laminin-1 may be of marked benefit to the stability of the myofibers. In addition, Vachon et al. (1996) reported only an increase in survival of myotubes with α2-laminin and not a decrease in survival with laminin-1 in normal myotubes. So although α2-

laminin has beneficial effects, laminin-1 is not necessarily detrimental to survival. The increased expression of α2-laminin mRNA and laminin-1 protein may contribute to the observed increase in strength, in addition to decreased fiber degeneration, and increased new myotube formation with treatment (Anderson et al., 1996). New fibers formed during treatment maybe more stable due to this action of deflazacort.

In the present study we have observed an increase in the proliferative proportion of differentiating mpcs (myogenin+) with deflazacort. These differentiating mpcs will be the cells that are later responsible for the synthesis of different isoforms of laminin, and the increase in laminin with deflazacort may only be secondary to the increase in differentiating mpc. Alternatively deflazacort itself may be increasing the expression of laminin in these cells facilitating the differentiation process and latter remodeling since Simo et al. (1992) show there is a glucocorticoid response element on laminin. Whether the sequence starts with deflazacort increasing myogenin+ mpc proliferation, which increases laminin expression or works in the reverse order is not known. In addition, it is not known whether the expression of the different isoforms of laminin are from the same or different cells and at what point during regeneration the synthesis of these proteins begins. The present study has shown that α2-laminin mRNA is expressed not in mononuclear cells but in newly-formed myotubes (as seen by *in situ* hybridization). However, to address these questions and determine the relevant time course of expression of different isoforms of laminin, a study is first needed to determine if laminin-1 and α2-laminin are co-localized in the same cells.

Alternatively, the increases in mpc proliferation and laminin expression may be secondary to changes in some other aspect of the dystrophin-glycoprotein complex for

example (see section 2.3). The dystrophin-glycoprotein complex is of key importance to the stability of the sarcolemma. Laminin is linked to the dystrophin-glycoprotein complex and indeed induces clustering of this complex (Cohen et al., 1997). Therefore if deflazacort treatment produced an increase in any one of the many proteins in the complex, secondary increases in laminin expression could theoretically result from treatment, although this idea had not been tested. Therefore the question of whether deflazacort directly or indirectly increases laminin expression is only the first question. If increased laminin expression is secondary to changes in components of the dystrophin-glycoprotein complex, an experiment could be performed to investigate whether or not component proteins are up- or down-regulated with deflazacort treatment. A more complete characterization of the different isoforms of laminin expressed during muscle regeneration and the time course of their expression would be important to further our understanding of the actions of deflazacort therapy on dystrophin-deficient muscle.

6.3 Summary

We have demonstrated that deflazacort treatment increases strength in *mdx* mice at least as a result of changes in the proportion of myogenin+ mpc proliferation and laminin-1 protein and α2-laminin mRNA expression (see section 6.2). We have attributed consequent potential gain in function to contributions of these and other structural changes. During 4 weeks of deflazacort treatment we observed an increase in grip strength in dystrophic *mdx* mice. In addition, strength got higher even after a short 2 week treatment period and was again higher than in the placebo-treated group some 6 weeks after treatment. The initial increase in strength with deflazacort treatment was

likely a result of previously reported changes in muscle repair and fiber diameter (Anderson et al., 1996) with contributions from increases in the proportion ofmyogenin+ mpc proliferation and α2-laminin mRNA and laminin-1 protein expression. The remaining beneficial effects immediately following treatment with deflazacort (1 week post-treatment) may be attributed to the continuation of these processes. However, the later increase in strength apparent at 6 weeks post-treatment may be related to the previous findings of our lab. Anderson et al. (1996) demonstrated deflazacort had both short and long term myogenic effects on repair. Deflazacort not only increased fusion of proliferative mpc, but also increased long term myotube growth and increased the populations of c-met+ satellite cells on regenerated fibers (Anderson, unpublished data). It is plausible that treatment with deflazacort caused an initial increase in the recruitment of satellite cells to the cell cycle and subsequent fusion. This could enable a later increase in myotube growth and the increase in strength long after treatment had ended.

The gains in strength of *mdx* mice on deflazacort treatment were measured over a period of time. By comparison, the effects of deflazacort on structure and differentiation were examined at one time point, 4 days after the crush injury. Regeneration is a long process of at least 14 days with many different signaling cascades that occur in a time-dependent manner. The chances of seeing the effects of treatment were maximized by selecting an important time interval in repair (4 days after crush), when proliferation and myotube formation are both at a peak. Deflazacort was observed to increase the expression of two different isoforms of laminin in dystrophin-deficient *mdx* mice. This demonstrated that the treatment had diverse effects and suggests a dynamic capability of muscle to compensate for the adverse effects of the lack of dystrophin. Further

investigation of the deflazacort-induced effects throughout regeneration (e.g. on the expression of molecules in the dystrophin-glycoprotein complex, with its crucial role in maintaining the structural integrity of muscle fibers) are now needed. The proliferative proportion of mpc was increased with deflazacort, particularly in those cells expressing mRNA for myogenin, the MRF gene responsible for initiating myogenic differentiation. While the signaling mechanisms responsible for the initial expression of MRFs have yet to be determined, the specific interactions of myogenin with glucocorticoid receptors in muscle or possibly mpc nuclei are likewise unknown. The present results suggest this information would be valuable in improving treatment for neuromuscular diseases where muscle repair would improve the outcome. In an attempt to determine the structural effects of deflazacort and reasons for the observed increases in strength with treatment, further investigation of the time course of changes at the molecular level have next to be elucidated in the process of regeneration.

The following specific conclusions can be made from this study.

1. The strength of muscles increased with deflazacort treatment as compared to placebo.
2. The proliferative proportion of myogenin+ but not MyoD+ mpc increased with deflazacort treatment.
3. With deflazacort treatment, CK isoform levels in regenerating muscle shifted to more mature MB and MM isoforms than in muscle from placebo-treated mice.
4. With deflazacort treatment, α2-laminin mRNA levels increased in all four muscle samples, but were increased relative to MM CK activity only in RTA, LTA and heart.
5. With deflazacort treatment, laminin-1 protein expression increased in all four muscles both as a proportion of muscle weight and relative to MM CK activity.

References

Albelda SM. Role of integrins and other cell adhesion molecules in tumor progression and metastasis. *Lab Invest* 68(1):4-17; 1993.

Allamand V, Sunada Y, Salih MA, Straub V, Ozo CO, Al-Turaiki MH, Akbar M, Kolo T, Colognato H, Zhang X, Sorokin LM, Yurchenco PD, Tryggvason K, Campbell KP. Mild congenital muscular dystrophy in two patients with an internally deleted laminin alpha2-chain. *Hum Mol Genet* 6(5):747-752; 1997.

Amalfitano A, Chamberlain JS. The mdx-amplification-resistant mutation system assay, a simple and rapid polymerase chain reaction-based detection of the *mdx* allele. *Muscle Nerve* 19(12):1549-1553; 1996.

Anderson JE, Bressler BH, Ovalle WK. Functional regeneration in the hindlimb skeletal muscle of the *mdx* mouse. *J Muscle Res Cell Motil* 9:499-515; 1988.

Anderson JE, Garrett K, Moor A, McIntosh L, Penner K. Dystrophy and myogenesis in *mdx* diaphragm muscle. *Muscle Nerve* 21(9):1153-1165; 1998.

Anderson JE, Liu L, Kardami E. Distinctive patterns of basic fibroblast growth factor (bFGF) distribution in degenerating and regenerating areas of dystrophic (*mdx*) striated muscles. *Dev Biol* 147:96-109; 1991.

Anderson JE, McIntosh LM, Poettcker R. Deflazacort but not prednisone improves both muscle repair and fiber growth in diaphragm and limb muscle in the *mdx* dystrophic mouse. *Muscle Nerve* 19:1576-1585; 1996.

Anderson JE, Ovalle WK, Bressler BH. Electron microscopic characterization of hindlimb muscle regeneration in the *mdx* mouse. *Anat Rec* 219:243-257; 1987.

Anderson JE. Murray L. Barr Award Lecture. Studies of the dynamics of skeletal muscle regeneration: the mouse came back! *Biochem Cell Biol* 76(1):13-26; 1998.

Angelini C, Pegoraro E, Turella E, Intino MT, Pini A, Costa C. Deflazacort in duchenne dystrophy: study of long-term effect. *Muscle Nerve* 17:386-391; 1994.

Angoli D, Corona P, Baresi R, Mora M, Wanke E. Laminin-alpha2 but not -alpha1-mediated adhesion of human (Duchenne) and murine (mdx) dystrophic myotubes is seriously defective. *FEBS Lett* 408(3):341-344; 1997.

Arnold HH, Winter B. Muscle differentiation: more complexity to the network of myogenic regulators. *Curr Opin Genet Dev* 8(5):539-544; 1998.

Bessman SP, Carpenter CL. The creatine-creatine phosphate energy shuttle. *Ann Rev Biochem* 54:831-862; 1985.

Bhagwati S, Ghatpande A, Shafiq SA, Leung B. *In situ* hybridization analysis for expression of myogenic regulatory factors in regenerating muscle of mdx mouse. *J Neuropathol Exp Neurol* 55(5):509-514; 1996.

Bischoff R, Heintz C. Enhancement of skeletal muscle regeneration. *Dev Dyn* 201:41-54; 1994.

Bischoff R. In: "*Myology*," Engel, A. and Franzini-Armstrong, C. (eds). New York: Mc-Graw Hill, pp. 97-118; 1994.

Bischoff R. Interaction between satellite cells and skeletal muscle fibers. *Development* 109(4):943-952; 1990.

Bressler BH, Jasch LG, Ovalle WK, Slonecker CE. Chances in isometric contractile properties of fast-twitch and slow-twitch skeletal muscle of C57BL/6J dy2J/dy2J dystrophic mice during postnatal development. *Exp Neurol* 80:457-470; 1983.

Brooke MH, Fenichel GM, Griggs RC, Mendell JR, Moxley RT 3d, Miller JP, Kaiser KK, Florence JM, Pandya S, Signore L. Clinical investigation of Duchenne muscular dystrophy. Interesting results in a trial of prednisone. *Arch Neurol* 44:812-817; 1987.

Brooke MH, Fenichel GM, Griggs RC, Mendell JR, Moxley R, Miller JP, Province MA. Clinical investigation in Duchenne dystrophy: 2. Determination of the "power of therapeutic trials based on the natural history. *Muscle Nerve* 6(2):91-103; 1983.

Brown SC, Lucy JA. Dystrophin as a Mechanochemical Transducer in Skeletal Muscle. *Bioessays* 15:413-419; 1993.

Brussee V, Tardif F, Tremblay JP. Muscle fibers of mdx mice are more vulnerable to exercise than those of normal mice. *Neuromuscul Disord* 7(8):487-492; 1997.

Bulfield G., W. Silver, P. Wright, K. Moore. X chromosome-linked muscular dystrophy (mdx) in the mouse. *Proc Natl Acad Sci U S A* 81:1189-1192; 1984.

Carpenter S, Karpati G. Segmental necrosis and its demarcation in experimental micropuncture injury of skeletal muscle fibers. *J Neuropathol Exp Neurol* 48(2):154-170; 1989.

Chambers RL, McDermott JC. Molecular basis of skeletal muscle regeneration. *Can J Appl Physiol* 21(3):155-184; 1996.

Chen G, Quinn LS. Partial characterization of skeletal myoblast mitogens in mouse crushed muscle extract. *J of Cell Physiol* 153(3):563-574; 1992.

Cho M, Hughes SM, Karsch-Mizrachi I, Travis M, Leinwand LA, Blau HM. Fast myosin heavy chains expressed in secondary mammalian muscle fibers at the time of their inception. *J Cell Sci* 107 (Pt 9):2361-2371; 1994.

Chomczynski P, Sacchi N. Single-step method of RNA isolation by acid guanidinium thiocyanate-phenol-chloroform extraction. *Anal Biochem* 162(1):156-159; 1987.

Cohen MW, Jacobson C, Yurchenco PD, Morris GE, Carbonetto S. Laminin-induced clustering of dystroglycan on embryonic muscle cells: comparison with agrin-induced clustering. *J Cell Biol* 136(5):1047-1058; 1997.

Cornelison DD, Wold BJ. Single-cell analysis of regulatory gene expression in quiescent and activated mouse skeletal muscle satellite cells. *Dev Biol* 191(2):270-283; 1997.

Dangain J, Vrbova G. Muscle development in mdx mutant mice. *Muscle Nerve* 7:700-704; 1984.

Davis RL, Cheng PF, Lassar AB, Weintraub H. The MyoD DNA binding domain contains a recognition code for muscle-specific gene activation. *Cell* 60(5):733-746; 1990.

Davis RL, Weintraub H, Lassar AB. Expression of a single transfected cDNA converts fibroblasts to myoblasts. *Cell* 51(6):987-1000; 1987.

Decary S, Mouly V, Butler-Browne GS. Telomere length as a tool to monitor satellite cell amplification for cell-mediated gene therapy. *Hum Gene Ther* 7(11):1347-1350; 1996.

Dias P, Dilling M, Houghton P. The molecular basis of skeletal muscle differentiation. *Semin Diagn Pathol* 11(1):3-14; 1994.

Drachman DB, Toyka KV, Myer E. Prednisone in Duchenne muscular dystrophy. *Lancet* 2(7894):1409-1412; 1974.

Dupont-Versteegden EE, McCarter RJ, Katz MS. Voluntary exercise decreases progression of muscular dystrophy in diaphragm of mdx mice. *J Appl Physiol* 77:1736-1741; 1994.

Duxson MJ, Usson Y, Harris AJ. The origin of secondary myotubes in mammalian skeletal muscles: ultrastructural studies. *Development* 107(4):743-750; 1989.

Ebashi SY, Toyokura HM, Sugita H. High creatine phosphokinase activity of sera of progressive muscular dystrophy patients. *J Biochem* 46:103-104; 1959.

Echtermeyer F, Sch¨ober S, P¨oschl E, von der Mark H, von der Mark K. Specific induction of cell motility on laminin by alpha 7 integrin. *J Biol Chem* 271(4):2071-2075; 1996.

Ehrig K, Leivo I, Argraves WS, Ruoslahti E, Engvall E. Merosin, a tissue-specific basement membrane protein, is a laminin-like protein. *Proc Natl Acad Sci U S A* 87(9):3264-3268; 1990.

Engel AG, Biesecker G. Complement activation in muscle fiber necrosis: demonstration of the membrane attack complex of complement in necrotic fibers. *Ann Neurol* 12(3):289-296; 1982.

Engvall E, Davis GE, Dickerson K, Ruoslahti E, Varon S, Manthorpe M. Mapping of domains in human laminin using monoclonal antibodies: localization of the neurite-promoting site. *J Cell Biol* 103(6 Pt 1):2457-2465; 1986.

Engvall E, Earwicker D, Haaparanta T, Ruoslahti E, Sanes JR. Distribution and isolation of four laminin variants; tissue restricted distribution of heterotrimers assembled from five different subunits. *Cell Regul* 1(10):731-740; 1990.

Engvall E, Wewer UM. Domains of laminin. *J Cell Biochem* 61:493-501; 1995.

Ervasti JM, Ohlendieck K, Kahl SD, Gaver MG, Campbell KP. Deficiency of a glycoprotein component of the dystrophin complex in dystrophic muscle. *Nature* 345:315-319; 1990.

Fenichel GM, Florence JM, Pestronk A, Mendell JR, Moxley RT 3d, Griggs RC, Brooke MH, Miller JP, Robison J, King W, Signore L, Pandya S, Schierbecker J, Wilson B. Long-term benifit from prednisone therapy in Duchenne muscular dystrophy. *Neurology* 41:1874-1877; 1991.

Ferrari G, Cusella-De Angelis G, Coletta M, Paolucci E, Stornaiuolo A, Cossu G, Mavilio F. Muscle regeneration by bone marrow-derived myogenic progenitors. *Science* 279:1528-1530; 1998.

Floyd SS Jr, Clemens PR, Ontell MR, Kochanek S, Day CS, Yang J, Hauschka SD, Balkir L, Morgan J, Moreland MS, Feero GW, Epperly M, Huard J. Ex vivo gene transfer using adenovirus-mediated full-length dystrophin delivery to dystrophic muscles. *Gene Ther* 5(1):19-30; 1998.

Garrett KL, Anderson JE. Colocalization of bFGF and the myogenic regulatory gene myogenin in dystrophic mdx muscle precursor and young myotubes in vivo. *Dev Biol* 169:596-608; 1995.

Gee SH, Blacher RW, Douville PJ, Provost PR, Yurchenco PD, Carbonetto S. Laminin-binding protein 120 from brain is closely related to the dystrophin-associated glycoprotein,

dystroglycan, and binds with high affinity to the major heparin binding domain of laminin. *J Biol Chem* 268(20):14972-14980; 1993.

Gee SH, Montanaro F, Lindenbaum MH, Carbonetto S. Dystroglycan-alpha, a dystrophin-associated glycoprotein, is a functional agrin receptor. *Cell* 77(5):675-686; 1994.

Goodman SL, Risse G, von der Mark K. The E8 subfragment of laminin promotes locomotion of myoblasts over extracellular matrix. *J Cell Biol* 109(2):799-809; 1989.

Gramolini AO, Jasmin BJ. Molecular mechanisms and putative signaling events controlling utrophin expression in mammalian skeletal muscle fibres. *Neuromuscul Disord* 8(6):351-361; 1998.

Gray RE, Doherty SM, Galloway J, Coulton L, de Broe M, Kanis JA. A double blind study of deflazacort and prednisone in patients with chronic inflammatory disorders. *Arthritis Rheum* 34:287-295; 1991.

Grounds MD, Garrett KL, Lai MC, Wright WE, Beilharz MW. Identification of skeletal muscle precursor cells in vivo by use of MyoD1 and myogenin probes. *Cell Tissue Res* 267(1):99-104; 1992.

Grounds MD, McGeachie JK. A model of myogenesis in vivo, derived from detailed autoradiographic studies of regenerating skeletal muscle, challenges the concept of quantal mitosis. *Cell Tissue Res* 250(3):563-569; 1987.

Grounds MD. Age-associated changes in the response of skeletal muscle cells to exercise and regeneration. *Ann N Y Acad Sci* 854:78-91; 1998.

Grounds MD. Phagocytosis of necrotic muscle in muscle isografts is influenced by the strain, age and sex of host mice. *J Pathol* 153:71-82; 1987.

Grounds MD. Towards understanding skeletal muscle regeneration. *Path Res Pract* 187:1-22; 1991.

Grounds MD, Yablonka-Reuveni Z. Molecular and cell biology of skeletal muscle regeneration. *Mol Cell Biol Hum Dis Ser* 3:210-256; 1993.

Hahn A, Bach JR, Delaubier A, Renardel-Irani A, Guillou C, Rideau Y. Clinical implications of maximal respiratory pressure determinations for individuals with Duchenne muscular dystrophy. *Arch Phys Med Rehabil* 78(1):1-6; 1997.

Hall PA, Levison DA. Review: assessment of cell proliferation in histological material. *J Clin Pathology* 43(3):184-92; 1990.

Hasard TH. *Understanding biostatistics*. Mosby-Year Book, St. Louis, Missouri, 1991.

Haushka S. The embryological origin of muscle. In: "*Myology*," Engel, A. and Franzini-Armstrong, C. (eds). New York: Mc-Graw Hill, pp. 3-73; 1994.

Hayes A, Williams DA. Beneficial effects of voluntary wheel running on the properties of dystrophic mouse muscle. *J Appl Physiol* 80(2):670-679; 1996.

Helbling-Leclerc A, Zhang X, Topaloglu H, Cruaud C, Tesson F, Weissenbach J, Tome FM, Schwartz K, Fardeau M, Tryggvason K, Guicheney P. Mutations in the laminin α2-chain gene (LAMA2) cause merosin-deficient congenital muscular dystrophy. *Nat Genet* 11:216-218; 1995.

Henry MD, Campbell KP. A role for dystroglycan in basement membrane assembly. *Cell* 95:859-870; 1998.

Hoffman EP, Morgan JE, Watkins SC, Partridge TA. Somatic reversion/suppression of the mouse *mdx* phenotype in vivo. *J Neurol Sci* 99:9-25; 1990.

Hudecki MS, Pollina CM, Granchelli JA, Daly MK, Byrnes T, Wang JC, Hsiao JC. Strength and endurance in the therapeutic evaluation of prednisolone-treated mdx mice. *Res Commun Chem Pathol Pharmacol* 79:45-60; 1993.

Hughes SM, Blau HM. Migration of myoblasts across basal lamina during skeletal muscle development. *Nature* 345(6273):350-353; 1990.

Huxley HE. Electron microscopic studies on the structure of natural and synthetic protein filaments from striated muscle. *J Mol Biol* 7:281-308; 1963.

Ibraghimov-Beskrovnaya O, Ervasti JM, Leveille CJ, Slaughter CA, Sernett SW, Campbell KP. Primary structure of dystrophin-associated glycoproteins linking dystrophin to the extracellular matrix. *Nature* 355:696-702; 1992.

Ikeda K, Mitsumoto H. *In vivo* and *in vitro* muscle tension in wobbler mouse motor neuron disease. *Muscle Nerve* 16:979-981; 1993.

Inui K, Okada S, Dickson G. Gene therapy in Duchenne muscular dystrophy. *Brain Development* 18(5):357-361; 1996.

Kadesch T. Helix-loop-helix proteins in the regulation of immunoglobulin gene transcription. *Immunol Today* 13:31-36; 1992.

Kami K, Noguchi K, Senba E. Localization of myogenin, c-fos, c-jun, and muscle-specific gene mRNAs in regenerating rat skeletal muscle. *Cell Tissue Res* 280(1):11-9; 1995.

Kardami E, Spector D, Strohman RC. Heparin inhibits skeletal muscle growth in vitro. *Dev Biol* 126(1):19-28; 1988.

Kelly AM, Zacks SI. The histogenesis of rat intercostal muscle. *J Cell Biol* 42:135-153; 1969.

Keynes R, Stern C. Mechanism of vertebrate segmentation. *Development* 103:413-429; 1988.

Khan MA. Corticosteroid therapy in Duchenne muscular dystrophy. *J Neurol Sci* 120:8-14; 1993.

Kuby SA, Keutel HJ, Okabe K, Jacobs HK, Ziter F, Gerber D, Tyler FH. Isolation of the human ATP-creatine transphosphorylases (creatine phosphokinases) from tissues of patients with Duchenne muscular dystrophy. *J Biol Chem* 252(23):8382-8390; 1977.

Kühl U, Ocalan M, Timpl R, von der Mark K. Role of laminin and fibronectin in selecting myogenic versus fibrogenic cells from skeletal muscle cells in vitro. *Dev Biol* 117(2):628-635; 1986.

Kühl U, Timpl R, von der Mark K. Synthesis of type IV collagen and laminin in cultures of skeletal muscle cells and their assembly on the surface of myotubes. *Dev Biol* 93(2):344-354; 1982.

Lawson-Smith MJ, McGeachie JK. Experimental skeletal muscle grafts as a model of regeneration. *Aust N Z J Surg* 67(1):35-9; 1997.

Leeuwenburgh C, Ji L. Glutathione depletion in rested and exercised mice: biochemical consequence and adaptation. *Arch Biochem Biophys* 316:941-949; 1995.

Lim LE, Campbell KP. The sarcoglycan complex in limb-girdle muscular dystrophy. *Curr Opin Neurol* 11(5):443-452; 1998.

Liotta LA, Rao CN, Wewer UM. Biochemical interactions of tumor cells with the basement membrane. *Annu Rev Biochem* 55:1037-57; 1986.

LoCascio V, Ballanti P, Milani S, Bertoldo F, LoCascio C, Zanolin EM, Bonucci E. A histomorphometric long-term longitudinal study of trabecular bone loss in glucocorticoid-treated patients: prednisone versus deflazacort. *Calcif Tissue Int* 62(3):199-204; 1998.

Lord JP, Portwood MM, Lieberman JS, Fowler WM Jr, Berck P. Upper extremity functional rating for patients with Duchenne muscular dystrophy. *Arch Phys Med Rehabil* 68(3):151-154; 1987.

Lough J, Bischoff R. Differentiation of creatine phosphokinase during myogenesis: quantitative fractionation of isozymes. *Dev Biol* 57(2):330-344; 1977.

Love DR, Hill DF, Dickson G, Spurr NK, Byth BC, Marsden RF, Walsh FS, Edwards YH, Davies KE. An autosomal transcript in skeletal muscle with homology to dystrophin. *Nature* 339(6219):55-8; 1989.

Lyons GE, Mühlebach S, Moser A, Masood R, Paterson BM, Buckingham ME, Perriard JC. Developmental regulation of creatine kinase gene expression by myogenic factors in embryonic mouse and chick skeletal muscle. *Development* 113:3 1017-1029; 1991.

Martin GR, Timpl R. Laminin and other basement membrane components. *Annu Rev Cell Biol* 3:57-85; 1987.

McGeachie JK, Grounds MD. Initiation and duration of muscle precursor replication after mild and severe injury to skeletal muscle of mice. An autoradiographic study. *Cell Tissue Res* 248(1):125-130; 1987.

McIntosh LM, Anderson JE. Hypothyroidism prolongs and increases mdx muscle precursor proliferation and delays myotube formation in normal dystrophic limb muscle. *Biochem Cell Biol* 73(3-4):181-190; 1995.

McIntosh LM, Garrett KL, Megeney L, Rudnicki MA, Anderson JE. Regeneration and myogenic cell proliferation correlate with taurine levels in dystrophin- and MyoD-deficient muscles. *Anat Rec* 252(2):311-324; 1998.

McIntosh LM, Pernitsky AN, Anderson JE. The effects of altered metabolism (hypothyroidism) on muscle repair in the mdx dystrophic mouse. *Muscle Nerve* 17(4):444-453; 1994.

McLennan IS. Neurogenic and myogenic regulation of skeletal muscle formation: a critical re-evaluation. *Prog Neurobiol* 44(2):119-140; 1994.

Megeney LA, Kablar B, Garrett K, Anderson JE, Rudnicki MA. MyoD is required for myogenic stem cell function in adult skeletal muscle. *Genes Dev* 10(10):1173-1183; 1996.

Megeney LA, Rudnicki MA. Determination versus differentiation and the MyoD family of transcription factors. *Biochem Cell Biol* 73(9-10): 723-732; 1995.

Mendell JR, Moxley RT, Griggs RC, Brooke MH, Fenichel GM, Miller JP, King W, Signore L, Pandya S, Florence J. Randomized, double-blind six-month trial of prednisone in Duchenne's muscular dystrophy. *N Engl J Med* 320(24):1592-1597; 1989.

Mesa LE, Dubrovsky AL, Corderi J, Marco P, Flores D. Steroids in duchenne muscular dystrophy: deflazacort trial. *Neuromuscul Disord* 1:161-166; 1991.

Metzinger L, Passaquin AC, Vernier A, Thiriet N, Warter JM, Poindron P. Lazaroids enhance skeletal myogenesis in primary cultures of dystrophin-deficient *mdx* mice. *J Neurol Sci* 126(2):138-145; 1994.

Meyer OA, Tilson HA, Byrd WC, Riley MT. A method for the routine assessment of fore- and hindlimb grip strength of rats and mice. *Neurobehav Toxicol* 1:233-236; 1979.

Miller RG, Sharma KR, Pavlath GK, Gussoni E, Mynhier M, Lanctot AM, Greco CM, Steinman L, Blau HM. Myoblast implantation in Duchenne muscular dystrophy: the San Francisco study. *Muscle Nerve* 20(4):469-478; 1997.

Mitchell CA, McGeachie JK, Grounds MD. Cellular differences in the regeneration of murine skeletal muscle: a quantitative histological study in SJL/J and BALB/c mice. *Cell Tissue Res* 269(1):159-166; 1992.

Montarras D, Chelly J, Bober E, Arnold H, Ott MO, Gros F, Pinset C. Developmental patterns in the expression of Myf5, MyoD, myogenin, and MRF4 during myogenesis. *New Biol* 3(6):592-600; 1991.

Morris GE. The use of creatine kinase activity as an index of skeletal-muscle differentiation. *Biochem Soc Trans* 6(3):509-511; 1978.

Moxley RT 3d. Functional testing. *Muscle Nerve* 13 Suppl:S26-9; 1990.

Mundegar R, von Oertzen J, Zierz S. Increased laminin A expression in regenerating myofibers in neuromuscular disorders. *Muscle Nerve* 18:992-999; 1995.

Nonaka I. Animal models of muscular dystrophies. *Lab Animal Sci* 48(1):8-17; 1998.

Ocalan M, Goodman SL, K¨uhl U, Hauschka SD, von der Mark K. Laminin alters cell shape and stimulates motility and proliferation of murine skeletal myoblasts. *Dev Biol* 125(1):158-167; 1988.

O'Connell SL, Tresham J, Fortune CL, Farrugia W, McDougall JG, Scoggins BA, Wark JD. Effects of prednisone and deflazacort on osteocalcin metabolism in sheep. *Calcif Tissue Int* 53:117-121; 1993.

Ohlendieck K, Campbell KP. Dystrophin-associated proteins are greatly reduced in skeletal muscle from *mdx* mice. *J Cell Biol* 115:1685-1694; 1991.

Ohlendieck K. Towards an understanding of the dystrophin-glycoprotein complex: linkage between the extracellular matrix and the membrane cytoskeleton in muscle fibers. *Eur J Cell Biol* 69(1):1-10; 1996.

Olson EN. Interplay between proliferation and differentiation within the myogenic lineage. *Dev Biol* 154(2):261-272; 1992.

Papadimitriou JM, Robertson TA, Mitchell CA, Grounds MD. The process of new plasmalemma formation in focally injured skeletal muscle fibers. *J Struct Biol* 103(2):124-134; 1990.

Partridge TA, Davies KE. Myoblast-based gene therapies. *British Medical Bullatin* 51:123-137; 1995.

Passaquin AC, Metzinger L, Leger JJ, Warter JM, Poindron P. Prednisone enhances myogenesis and dystrophin-related protein in skeletal muscle cell cultures from *mdx* mouse. *J Neurosci Res* 35:363-372; 1993.

Pedemonte M, Sandri C, Schiaffino S, Minetti C. Early decrease of IIx myosin heavy chain transcripts in Duchenne muscular dystrophy. *Biochem Biophys Res Commun* 255(2):466-469; 1999.

Pernitsky AN, Anderson JE. Differential effects of 3,5,3'-triiodothyronine on control and mdx myoblasts and fibroblasts: analysis by flow cytometry. *Exp Cell Res* 227(2):214-222; 1996.

Petrof BJ. The molecular basis of activity-induced muscle injury in Duchenne muscular dystrophy. *Mol Cell Biochem* 179(1-2):111-123; 1998.

Pin CL, Ludolph DC, Cooper ST, Klocke BJ, Merlie JP, Konieczny SF. Distal regulatory elements control MRF4 gene expression in early and late myogenic cell populations. *Dev Dyn* 208(3):299-312; 1997.

Podhorska-Okolow M, Sandri M, Zampieri S, Brun B, Rossini K, Carraro U. Apoptosis of myofibres and satellite cells: exercise-induced damage in skeletal muscle of the mouse. *Neuropathol Appl Neurobiol* 24(6):518-531; 1998.

Rantanen J, Hurme T, Lukka R, Heino J, Kalimo H. Satellite cell proliferation and the expression of myogenin and desmin in regenerating skeletal muscle: evidence for two different populations of satellite cells. *Lab Invest* 72:3 341-347; 1995.

Roberts P, McGeachie JK, Grounds MD, Smith ER. Initiation and duration of myogenic precursor cell replication in transplants of intact skeletal muscles: an autoradiographic study in mice. *Anat Rec* 224(1):1-6; 1989.

Roberts RG, Coffey AJ, Bobrow M, Bentley DR. Determination of the exon structure of the distal portion of the dystrophin gene by vectorette PCR. *Genomics* 13(4):942-950; 1992.

Robertson TA, Grounds MD, Mitchell CA, Papadimitriou JM. Fusion between myogenic cells in vivo: an ultrastructural study in regenerating murine skeletal muscle. *J Struct Biol* 105(1-3):170-182; 1990.

Robertson TA, Maley MAL, Grounds MD, Papadimitriou JM. The role of macrophages in skeletal muscle regeneration with particular reference to chemotaxis. *Exp Cell Res* 207:321-331; 1993.

Rudnicki MA, Jaenisch R. The MyoD family of transcription factors and skeletal myogenesis. *Bioessays* 17(3):203-309; 1995.

Rudnicki MA, Schnegelsberg PN, Stead RH, Braun T, Arnold HH, Jaenisch R. MyoD or Myf-5 is required for the formation of skeletal muscle. *Cell* 75(7):1351-1359; 1993.

Rueger B, Thalhammer J, Obermaier I, Gruenewald-Janho S. Experemental procedure for the detection of a rare human mRNA with the DIG system. *Biochemica* 3:35-38; 1996.

Russell JC, Epling WF, Pierce D, Amy RM, Boer DP. Induction of voluntary prolonged running by rats. *J Appl Physiol* 63:2549-2553; 1987.

Schleimer RP. An overview of glucocorticoid anti-inflammatory actions. *J Clin Pharmacol* 45 Suppl 1:S3-7, discussion S43-4; 1993.

Schultz E, McCormick KM. Skeletal muscle satellite cells. *Rev Physiol Biochem Pharmacol* 123:213-257; 1994.

Sewry CA, Chevallay M, Tome FM. Expression of laminin subunits in human fetal skeletal muscle. *Histochem J* 27:497-504; 1995.

Sewry CA, Philpot J, Mahony D, Wilson LA, Muntoni F, Dubowitz V. Expression of laminin subunits in congenital muscular dystrophy. *Neuromuscul Disord* 5(4):307-316; 1995.

Siegel IM, Miller JE, Ray RD. Failure of corticosteroid in the treatment of Duchenne (pseudo-hypertrophic) muscular dystrophy. Report of a clinically matched three year double-blind study. *IMJ Ill Medical Journal* 145(1):32-33. 1974.

Simo P, Simon-Assmann P, Arnold C, Kedinger M. Mesenchyme-mediated effect of dexamethasone on laminin in cocultures of embryonic gut epithelial cells and mesenchyme-derived cells. *J Cell Sci* 101 (Pt 1):161-71; 1992.

Sklar RM, Brown RH Jr. Methylprednisolone increases dystrophin levels by inhibiting myotube death during myogenesis of normal human muscle in vitro. *J Neurol Sci* 101(1):73-81; 1991.

Sobel ME. Differential expression of the 67 kDa laminin receptor in cancer. *Semin Cancer Biol* 4(5):311-7; 1993.

Song WK, Wang W, Foster RF, Bielser DA, Kaufman SJ. H36-alpha 7 is a novel integrin alpha chain that is developmentally regulated during skeletal. *J Cell Biol* 117(3):643-57; 1992.

Song WK, Wang W, Sato H, Bielser DA, Kaufman SJ. Expression of alpha 7 integrin cytoplasmic domains during skeletal muscle development: alternate forms, conformational change, and homologies with serine/threonine kinases and tyrosine phosphatases. *J Cell Sci* 106 (Pt 4):1139-52; 1993.

Squire JM. Architecture and function in the muscle sarcomere. *Curr Opin Struct Biol* 7(2):247-257; 1997.

Staron RS. Human skeletal muscle fiber types: delineation, development, and distribution. *Can J Appl Physiol* 22(4):307-327; 1997.

Stedman HH, Sweeney HL, Shrager JB, Maguire HC, Panettieri RA, Petrof B, Narusawa M, Leferovich JM, Sladky JT, Kelly AM. The mdx mouse diaphragm reproduces the degenerative changes of Duchenne muscular dystrophy. *Nature* 352(6335):536-539; 1991.

Storch TG, Talley GD. Oxygen concentration regulates the proliferative response of human fibroblasts to serum and growth factors. *Exp Cell Res* 175(2):317-325; 1988.

Sunada Y, Edgar TS, Lotz BP, Rust RS, Campbell KP. Merosin-negative congenital muscular dystrophy associated with extensive brain abnormalities. *Neurology* 45:2084-2089; 1995.

Tatsumi R, Anderson JE, Nevoret CJ, Halevy O, Allen RE. HGF/SF is present in normal adult skeletal muscle and is capable of activating satellite cells. *Dev Biol* 194:114-128; 1998.

Tiger C, Gullberg D. Absence of laminin $\alpha 1$ chain in the skeletal muscle of dystrophic dy/dy mice. *Muscle Nerve* 20:1515-1524; 1997.

Torres LF, Duchen LW. The mutant *mdx*: inherited myopathy in the mouse. Morphological studies of nerves, muscles and end-plates. *Brain* 110:269-299; 1987.

Vachon PH, Loechel F, Xu H, Wewer UM, Engvall E. Merosin and laminin in myogenesis; specific requirement for merosin in myotube stability and survival. *J Cell Biol* 134(6):1483-1497; 1996.

Vachon PH, Xu H, Liu L, Loechel F, Hayashi Y, Arahata K, Reed JC, Wewer UM, Engvall E. Integrins (alpha7beta1) in muscle function and survival. Disrupted expression in merosin-deficient congenital muscular dystrophy. *J Clin Invest* 100(7):1870-1881; 1997.

von der Mark H, Dürr J, Sonnenberg A, von der Mark K, Deutzmann R. Goodman SL Skeletal myoblasts utilize a novel beta 1-series integrin and not alpha 6 beta 1 for binding to the E8 and T8 fragments of laminin. *J Biol Chem* 266(35):23593-601; 1991.

von der Mark K, Ocalan M. Antagonistic effects of laminin and fibronectin on the expression of the myogenic phenotype. *Differentiation* 40(2):150-157; 1989.

von der Mark K, Risse G. Isolation and characterization of laminin receptors. *Methods Enzymol* 144:490-507; 1987.

Watkins SC, Cullen MJ. A quantitative comparison of satellite cell ultrastructure in Duchenne muscular dystrophy, polymyositis and normal controls. *Muscle Nerve* 9:724-730; 1986.

Watkins SC, Cullen MJ. A quantitative study of myonuclear and satellite cell nuclear size in Duchenne muscular dystrophy, polymyositis and normal human skeletal muscle. *Anat Rec* 222:6-11; 1988.

Webster C, Blau HM. Accelerated age-related decline in replicative life-span of Duchenne muscular dystrophy myoblasts: implications for cell and gene therapy. *Somat Cell Mol Genet* 16:557-565; 1990.

Weintraub H, Davis R, Tapscott S, Thayer M, Krause M, Benezra R, Blackwell TK, Turner D, Rupp R, Hollenberg S. The myoD gene family: nodal point during specification of the muscle cell lineage. *Science* 251(4995):761-766; 1991.

Weintraub H, Tapscott SJ, Davis RL, Thayer MJ, Adam MA, Lassar AB, Miller AD. Activation of muscle-specific genes in pigment, nerve, fat, liver, and fibroblast cell lines by forced expression of MyoD. *Proc Natl Acad Sci U S A* 86(14):5434-5438; 1989.

Weintraub H. The MyoD family and myogenesis: redundancy, networks, and thresholds. *Cell* 75(7):1241-1244; 1993.

Weller B, Massa R, Karpati G, Carpenter S. Glucocorticoids and immunosuppressants do not change the prevalence of necrosis and regeneration in mdx skeletal muscles. *Muscle Nerve* 14(8):771-774; 1991.

Wewer UM, Engvall E. Laminins. *Methods in Enzymol* 245:85-104; 1994.

White TP, Esser KA. Satellite cell and growth factor involvement in skeletal muscle growth. *Med Sci Sports Exerc* 21(5 Suppl):S158-163; 1989.

Wilkinson D. *In situ hybridization: A practical approach*. Oxford University Press: Oxford. pp. 1-32; 1992.

Winder SJ. The membrane-cytoskeleton interface: the role of dystrophin and utrophin. *J Muscle Res Cell Motil* 18(6):617-629; 1997.

Wright WE, Sassoon DA, Lin VK. Myogenin, a factor regulating myogenesis, has a domain homologous to MyoD. *Cell* 56(4):607-617; 1989.

Xu H, Christmas P, Wu X, Wewer UM, Engvall E. Defective muscle basement membrane and lack of M-laminin in the dystrophic *dy/dy* mouse. *Proc Natl Acad Sci U S A* 91:5572-5576; 1994.

Yablonka-Reuveni Z, Seger R, Rivera AJ. Fibroblast growth factor promotes recruitment of skeletal muscle satellite cells in young and old rats. *J Histochem Cytochem* 47(1):23-42; 1999.

Yamashita K, Yoshioka T. Profiles of creatine kinase isoenzyme compositions in single muscle fibres of different types *J Muscle Res Cell Motil* 12(1):37-44; 1991.

Yun K, Wold B. Skeletal muscle determination and differentiation: Story of a core regulatory network and its context. *Curr Opin Cell Biol* 8:877-889; 1996.

Zacharias JM, Anderson JE. Muscle regeneration after imposed injury is better in younger than older mdx dystrophic mice. *J Neurol Sci* 104(2):190-196; 1991.

Ziter FA. Creatine kinase in developing skeletal and cardiac muscle of the rat. *Exp Neurol* 43(3):539-546; 1974.

Ziober BL, Vu MP, Waleh N, Crawford J, Lin CS, Kramer RH. Alternative extracellular and cytoplasmic domains of the integrin alpha 7 subunit are differentially expressed during development. *J Biol Chem* 268(35):26773-83; 1993.

Appendix

Solution D stock:

ddH_2O	293mL
4M guanidinium thiocyanate	250g
25mM sodium citrate (pH 7)	17.6mL 0.75M
0.5% sarcosyl	26.4mL of 10%

Solution D working:

0.1M 2-mercaptoethanol 360µl/50mL stock

Buffer 1:

	Makes – 2.5L	**Makes – 4.0L**
Maleic acid (100mM)	29.018g	46.428g
Sodium Chloride (150mM)	21.915g	35.064g
NaOH	~20g to pH 7.5	~30g to pH 7.5

Buffer 2:

	Makes - 100mL
1% blocking reagent in buffer 1	1g
10% stock	10g

* Heat to ~70°C to help blocking reagent dissolve and store aliquots at -20°C.

Buffer 3: (pH 9.5)

	Makes - 1.0L
100mM Tris	12.11g Tris base
100mM Sodium Chloride	33.3mL 3M or 20mL 5M or 5.844g
50mM Magnesium Chloride	50mL 1M or 10.165g

* If precipitate forms, filter solution.

Buffer 4: (pH 8.0)

	Makes - 1.0L
10mM Tris	10mL 1M
1mM EDTA	2mL 0.5M

Diethyl pyrocarbonate water (DEPC ddH_2O):

ddH_2O	1L
DEPC	1.0mL
absolute ethanol	9.0mL

- mix solution and let stand in fumehood overnight,
- autoclave.

Formaldehyde RNA Gel (1.2%): 100mL

Agarose	1.2g
DEPC ddH_2O	83.4mL

10x MOPS	10mL
37% Formaldehyde	6.6mL

RNA Sample Buffer:

	Amount needed	**Final Conc.**
Formamide	500µL	50%
10x MOPS	100µL	10% (1x)
37% Formaldehyde	175µL	17.5%
Ethidium Bromide (10mg/mL)	5µL	.5% (0.05µg/µL)
Sterile Glycerol	100µL	10%
Bromophenol Blue	2.5mg	.25%
Total Volume	1mL	

* wrap in aluminum foil and store at -20°C.

10x MOPS:

DEPC ddH_2O	800mL
Morpholinopropanesulfonic acid (0.2M)	41.8g
3M Sodium Acetate (DEPC) (50mM)	16.6mL
0.5M EDTA pH 8 (DEPC) (10mM)	20.0mL

- make up to 1L with DEPC ddH_2O, do not autoclave, and store at room temp.

0.5M ethylenediaminetetracetic acid (EDTA): (pH 8)

ddH_2O	800mL
EDTA	186.1g

- autoclave.

3M sodium acetate (NaAc): (pH 5.2)

ddH_2O	80mL
Sodium Acetate.3H_2O	40.81g

- pH to 5.2 with glacial acetic acid,
- makes up to 100mL,
- autoclave.

1M magnesium chloride ($MgCl_2$):

ddH_2O	1L
$MgCl_2.6H_2O$	203.3g

- autoclave.

5M sodium chloride (NaCl):

ddH_2O	500mL
NaCl	146.25g

1M Tris:

- add 121.1g Tris base to 800mL ddH_2O

pH	**Vol. of HCl**
7.4	70mL

7.6	60mL
8.0	42mL

10% sodium dodecyl sulfate (SDS): (pH 7)

ddH_2O	500mL
SDS	50g

20x standard saline citrate (SSC): (pH 7)

	Makes - 1L
ddH_2O	800mL
3M NaCl	175.3g
0.3M trisodium citrate	88.2g

- make up to 1L,
- autoclave.

Working solutions

10x SSC	300mL	20x SSC
	300mL	DEPC ddH_2O
6x SSC	150mL	20x SSC
	350mL	DEPC dH_2O
2x SSC	60mL	20x SSC
	540mL	DEPC ddH_2O

2x SSC 0.1% SDS:

20x SSC	100mL
10% SDS	1g or 10mL

- make up to 1L with DEPC ddH_2O,
- autoclave.

0.1x SSC 0.1% SDS:

20x SSC	5mL
10% SDS	1g or 10mL

- make up to 1L with DEPC ddH_2O,
- autoclave.

Hybridization Buffer for DIG-labeled probes:

	Amount	Final Conc.
Deionized formamide	25mL	50%
50% Dextran Sulfate	10mL	10%
20x SSC	12.5mL	5x
50x Denhardt's solution	2mL	2x
10% N-lauroyl sarcosine	0.5μL	0.1%
Boehringer Blocking Reagent	1g	2%

Formamide Deionization:

- add 5g Mixed Bed Resin Beads TMD-8 (Sigma) to 50mL falcon tubes,
- add formamide to falcon tubes. Shake and stir at 4°C overnight,

- let settle at 4°C for 2 hours,
- sterilize by using a Nalgene 0.45 μm vacuum filtration unit,
- store in new 50mL falcon tubes at -70°C.

50% Dextran Sulfate:

DEPC ddH_2O (68°C)	8.0mL
Dextran Sulfate	5.0g

- place in a warm water bath and then bring up to a final vol. of 10mL with DEPC ddH_2O
- use immediately.

Derhardt's Solution (50x):

Ficoll	5.0g
Polyvinylpyrrolidone	5.0g
Bovine Serum Albumin (BSA; 1%)	5.0g

- make up to 500mL with DEPC ddH_2O

12% Paraformaldehyde:

1x PBS	100mL
Paraformaldehyde	12g

- working solution (4%): dilute stock 1/3 with 1x PBS

10x phosphate buffered saline (PBS; pH 7.4):

	Makes - 1L
137mM NaCl	80g
2.7mM KCl	2g
10mM $Na_2HPO_4.7H_2O$	27.2g
1.76mM KH_2PO_4	2.4g

* at 4°C 10x PBS precipitates.

Primary Ab Dilutent (10mL):

0.01M PBS	9mL
BSA	0.1g
10% horse serum	1mL

Secondary Ab Dilutent (10mL):

0.01M PBS	10mL
BSA (1%)	0.1g

2.5M Tris-HCl Buffer: (pH 7.2)

ddH_2O	40mL
HCl (6N)	25mL
Tris Base	30.285g

- make up to 100mL with ddH_2O.

Separating Gel Preparation: 7.5%

ddH_2O	4.85mL

1.5M Tris-HCL, pH 8.8	2.5mL
10% (w/v) SDS stock (store at room temp.)	100µL
Acrylamide/Bis (30% stock) (Degas for >15 minutes at rt)	2.5mL
10% ammonium persulfate (fresh daily)	50µL
TEMED	5µL
Total	**10mL**

* 10% ammonium persulfate solution; dissolve 100mg APS in 1mL ddH_2O.

Stacking Gel Preparation: 4%

ddH_2O	6.1mL
0.5M Tris-HCl, pH 6.8	2.5mL
10% (w/v) SDS	100µL
Acrylamide/Bis (30% stock) (Degas for 15 minutes at room temperature)	1.3mL
10% ammonium persulfate (fresh daily)11	50µL
TEMED	10µL
Total	**10mL**

Sample Buffer (SDS reducing buffer):

ddH_2O	4.0mL
0.5 M Tris-HCl, pH 6.8	1.0mL
Glycerol	0.80mL
10% (w/v) SDS	1.6mL
2-β-mercaptoethanol	0.4mL
0.05% (w/v) bromophenol blue	0.2mL

* store at room temp.

5x Electrode (Running) Buffer: pH 8.3

Tris base	9g
Glycine	43.2g
SDS	3g
	To 600mL with ddH_2O

* store at 4°C and warm to 37°C before use if precipitation occurs.
1x Running buffer for one electrophoretic run; dilute 60mL 5x stock with 240mL ddH_2O.

Transfer Buffer: pH 8.3

Tris	25mM (3.03g)
Glycine	192mM (14.4g)

- make to 1L with ddH_2O

Coomassie Blue:

ddH_2O	250mL
Methanol	200mL
Glacial Acetic Acid	50mL

Comassie Blue	0.5g
De-stain:	
ddH_2O	250mL
Methanol	200mL
Glacial Acetic Acid	50mL
Blocking reagent:	
ddH_2O	38mL
Tris-HCl	0.299g
Tween 20	114µL
milk powder	1.9g
DAB Working Solution:	
1x PBS	50mL
DAB	10mg
colour intensifier	100µL
3% H_2O_2.	100µL
Colour intensifier:	
ddH_2O	10mL
$NiCl_2.6\ H_2O$ (5%)	0.5g
$CoCl_2.6\ H_2O$ (5%)	0.5g